

A NOVEL SPECIFICITY PROTEIN 1 (*SP1*)-LIKE GENE, REGULATING PROTEIN KINASE C-1 (*PKC1*)-DEPENDENT CELL-WALL INTEGRITY AND VIRULENCE FACTORS IN *CRYPTOCOCCUS NEOFORMANS*

Amos Adler^{1,2}, Yoon-Dong Park³, Peter Larsen⁴, Vijayaraj Nagarajan⁵, Kurt Wollenberg⁵, Jin Qiu³, Timothy G. Myers⁶ and Peter R. Williamson^{*2,3}

¹Department of Pediatrics, Section of Pediatric Infectious Disease, University of Chicago, Chicago, IL, USA.

²Section of Infectious Diseases, Department of Medicine, University of Illinois at Chicago College of Medicine, Chicago, IL, USA.

³Laboratory of Clinical Infectious Diseases, National Institute of Allergy and Infectious Diseases, National Institutes of Health, Bethesda, MD, USA

⁴Biosciences Division, Argonne National Laboratory, Lemont, IL, USA.

⁵Bioinformatics and Computational Biosciences Branch, Office of Cyber Infrastructure and Computational Biology, National Institute of Allergy and Infectious Diseases, National Institutes of Health, MD, USA

⁶Genomic Technologies Section, Research Technologies Branch, National Institute of Allergy and Infectious Diseases, National Institutes of Health, MD, USA

Address correspondence to: Peter R. Williamson, MD, PhD, 9000 Rockville Pike, Building 10, Rm 11N234, MSC 1888, Bethesda, MD 20892. Fax (301) 480-7321; e-mail: williamsonpr@mail.nih.gov

Eukaryotic cells utilize complex signaling systems to detect their environments, responding and adapting as new conditions arise during evolution. The basidiomycete fungus *Cryptococcus neoformans* is a leading cause of AIDS-related death worldwide and utilizes the calcineurin and protein kinase C-1 (Pkc1) signaling pathways for host adaptation and expression of virulence. In the present studies, a C-terminal zinc finger transcription factor, homologous to both the calcineurin responsive zinc fingers (Crz1) of ascomycetes and to the Pkc1 dependent specificity protein-1 (Sp1) transcription factors of metazoans, was identified and named *SP1* because of its greater similarity to the metazoan factors. Structurally, the Cn Sp1 protein was found to have acquired an additional Zn finger motif from that of Crz1 and showed Pkc1 dependent phosphorylation, nuclear localization and whole genome epistatic associations under starvation conditions. Transcriptional targets of Cn Sp1 shared functional similarities with Crz1 factors such as cell wall synthesis, but gained the regulation of processes involved in carbohydrate metabolism including trehalose metabolism and lost others such as the induction of autophagy. In addition, overexpression of Cn Sp1 in a *pkc1Δ* mutant showed restoration of altered phenotypes

involved in virulence including cell wall stability, nitrosative stress and extracellular capsule production. Cn Sp1 was also found to be important for virulence of the fungus using a mouse model. In summary, these data suggest an evolutionary shift in C-terminal Zn finger proteins during fungal evolution, transforming them from calcineurin-dependent to *PKC1*-dependent transcription factors, helping to shape the role of fungal pathogenesis of *Cryptococcus neoformans*.

The basidiomycete yeast *Cryptococcus neoformans* has emerged as one of the major causative agents of meningoencephalitis in immunocompromised hosts, such as persons with AIDS, organ transplant recipients, and patients receiving high doses of corticosteroid treatment. Systemic infections can also occur in immunocompetent individuals (1-2). As rates of infection have diminished in developed countries, attention is increasingly being focused on the high rates of cryptococcosis in the developing countries of Africa and Asia where cryptococcosis has been found to account for an estimated 17% of AIDS-related deaths (3). Recent studies have shown cryptococcosis to account for over 600,000 deaths annually, resulting in a disease burden worldwide approaching that of tuberculosis (4).

The 3 best-known virulence-associated traits of *C. neoformans* include: its ability to grow at 37°C (5), the presence of a copper-containing laccase that is capable of producing melanin pigments (6), and a high MW polysaccharide capsule (7-9). While temperature and capsule are likely to have multiple structural genes involved in expression, melanin production has been shown to be dependent on two laccase enzymes encoded by *LAC1* and *LAC2*, the former of which is the predominant enzyme under pathogenic conditions (6), making *LAC1* an excellent marker for studying virulence regulation in *C. neoformans*.

Yeast cells, including *C. neoformans*, are continuously exposed to a wide variety of environmental stresses in both their natural habitats and their resident hosts. These stresses include changes in temperature, osmolarity, pH, nutrients, and exposure to reactive oxygen and nitrogen molecules. They subsequently sense and react to these changes through a complex network of signal transduction pathways, thus adapting to their surroundings and ensuring repair of cellular damage. A major cellular pathway mediating these responses is the Protein Kinase C (*PKC1*) pathway. Within this pathway, activation of Pkc1 leads to sequential phosphorylation of a Mitogen-Activating Protein Kinase (MAPK) cascade, consisting of Bck1p, two redundant MAPK Kinases (Mkk1p and Mkk2p), and the MAPK, Slt2/Mpk1p (10). In *S. cerevisiae*, Rlm1p (11-14) and Swi4/Swi6 (15) are the main transcription factors (TF) responsible for Slt2/Mpk1p cell wall regulation. At least 25 genes that are involved in the biosynthesis of the cell wall and are regulated by Slt2/Mpk1p and Rlm1p have been described (11).

In *C. neoformans*, mutation of *PKC1* results in mutants that have profound cell wall integrity defects, including an inability to grow without the addition of an osmotic stabilizer such as sorbitol, and profound growth defects in the presence of various stressors. In addition, major virulence factors are altered in *pkc1Δ* strains, including an inability to grow in 37°C, aberrant capsule and decreased melaninogenesis (16). The phenotypic features of mutants of the major genes regulated by the Pkc1 pathway have also been characterized in *C. neoformans* including Bck1, Mkk2 and Mpk1 (16-17). However, while Pkc1 has been implicated in resistance to nitrosative stress and laccase

expression, the transcription factor(s) responsible for the signal from Pkc1 has not been identified.

In the present studies, we sought to characterize a C-terminal Zinc finger C2H2 type transcription factor protein, annotated *CNAG_00156* (Broad website; NCBI annotation XP_566613.1), that was first thought to represent a calcineurin-dependent Zn finger protein (Crz1), based on close homology to the *S. cerevisiae* and *Candida albicans* Crz1 homolog sequence. These studies were motivated by a previously-described role for the Ca²⁺ activated calcineurin pathway in cryptococcal virulence (5) and a role for calcium activation of laccase (18) as well as enzyme inhibition by the calcineurin inhibitor, FK506 (unpublished observation). However, to our surprise, we could not find evidence that *CNAG_00156* was part of the calcineurin pathway. Further studies to identify the relevant signal transduction pathway utilized a novel transcriptional clustering screen which identified Pkc1 as a likely signaling pathway for *CNAG_00156*. Biochemical and epistatic studies provided additional evidence linking the Pkc1 signal transduction pathway and the cryptococcal Zn finger transcription factor.

EXPERIMENTAL PROCEDURES

Strains, plasmids and media- Strains used in this study are detailed in Table S1. All strains were grown on YPD medium (1% yeast extract, 2% Bacto peptone, and 2% dextrose). Solid media contained 2% Bacto agar. All *PKC1* deletion strains were grown on YPD supplemented with 1 M sorbitol. Glucose starvation experiments were done as previously described (19). Selective media included either YPD containing 100 U/ml hygromycin B (InvivoGen) or asparagine minimal media as previously described (20). A modified Bluescript SK vector (Stratagene) with the 2.4-kb hygromycin-B resistance gene under the control of a cryptococcal actin promoter (21) was a gift of G. Cox (Duke University, Durham, North Carolina, USA). In addition to the cryptococcal shuttle vector pORA-KUT (19), a hygromycin B containing vector was generated by replacing the *URA5* transformation marker with the hygromycin-B resistance gene at the *KpnI* site, generating pORA-KUT (HygB). *Sequence data mining and analysis*-Sequence data was retrieved from the NCBI, Broad Institute website, and the SGD databases, for *H. sapiens*, *C.*

neoformans and *S. cerevisiae*, respectively. For the analysis of metazoan and fungal zinc finger motifs sequences were retrieved using BLASTp searches with human Sp1 and *C. neoformans* CNAG_00156 as the query sequences. Occasionally there were BLASTp hits to multiple zinc finger motifs in target sequences. For these cases the highest scoring hit was used as the putative homolog. The full protein sequences were aligned using MUSCLE (22) and the zinc finger motifs were manually extracted and aligned. A phylogenetic analysis of the zinc finger motifs (Fig. S3B) was performed using the heuristic parsimony algorithm of PAUP 4b10 (23). To evaluate support for the groups in the tree 500 nonparametric bootstrap replicates were analyzed. PAUP returned 500 equally parsimonious trees for which the 50% majority-rule consensus is shown. In Fig. 2B clades consisting of major taxonomic groups from Fig. S3B were collapsed when possible. All of the variation among the equally parsimonious trees occurred within these collapsed groups so the branches shown in the figure were found in all 500 trees.

Generation of Cn sp1Δ, and Cn sp1Δ:Cn SP1 strains- Standard methods were used for disruption and complementation of the *Cn SP1* (CNAG_00156) gene, as described previously (20). Briefly, to make the deletion construct, 2 PCR-amplified fragments of the *Cn SP1* homolog (using primers Crz1 S1 *Xba* I, 5'- GCTCTAGAATGGCAGATCCAGCCTCAC, and Crz1 500 A *Eco*R I, 5'- GGAATTCTGTTCGGACATCCTGCCTTC; Crz1 3171 S *Bgl* II, 5'- GAAGATCTCACAAG GCATTTTAATCTCAAGG, and Crz1 3693 A *Xho* I, 5'- CCGCTCGAGAATCCTCTTCACT CGTTTCACTC), the first digested with *Xba* I and *Eco*R I and the second digested with *Bgl* II and *Xho* I, were mixed with a 1.4-kb PCR fragment of the *URA5* gene described previously (20), digested with *Bgl* II and *Eco*R I and ligated to BlueScript SK digested with *Xba* I and *Xho* I. The final disruption allele with a 1.3-kb *URA5* marker flanked on either side by a 500-bp DNA sequence homologous to genomic regions of the *Cn SP1* gene was PCR-amplified and introduced into H99 *ura5* cells via a biolistic approach (21) to affect a 3.7-kb deletion within the *Cn SP1* coding region. Transformants were screened for potential *Cn SP1* deletion mutant by a PCR approach, and the specific disruption of the *Cn SP1* gene in candidate mutants was verified by Southern blot analysis and PCR of cDNA, to

verify the lack of *Cn SP1* transcription (Fig. S7). To complement the *Cn sp1Δ* mutant strain, a 5.7-kb genomic fragment encompassing the full ORF of *Cn SP1* plus ~1500 b.p. of the 5' promoter region and 500 b.p. of the 3'-UTR was PCR amplified using a primer set of Crz1 US -1500 *Bam* H I (5'- GCGGATCCATACACGAC AAACACATCGCTACA) and Crz1-500 3'UTR-A-*Bam*H I (5'- CGCGGATCCACGAT GAAAATGAAGGCTTCGACAATA) and then cloned into the modified pBluescript SK vector containing the hygromycin-B resistance gene to generate the complementation construct, which was introduced into *Cn sp1Δ* mutant cells by a biolistic approach. Transformants were selected on hygromycin- containing YPD agar plates. Genomic insertion of the wt *Cn SP1* construct in the complement was verified by uncut Southern blot.

Generation of constituent expression and GFP-tagged strains of PKC1 and Cn SP1-As the *Cn SP1* and *PKC1* genes contains *Eco*R I site, cloning into the pORA-KUT vector required additional restriction sites. An oligonucleotide poly-linker containing the following restriction sites (*Bgl*II-*Bam*HI-*Xba*I-*Nar*I-*Nhe*I-end codon-*Eco*RI) was inserted between the *Bgl* II and *Eco*R I sites of pORA-KUT. The ~730bp *C. neoformans* actin promoter (+/- *c-myc* tag) was amplified from H99 DNA using primers Actin promoter 1S *Bgl* II (5'- GGAAGATCTTGTCGGAGGAGAGGATGATGG TAAC), Actin promoter 730A *Bam* H I (5'- CGCGGATCCGTTGGGCGAGTTTACTAATGGA AAAAGA) or Actprmtr0A-Myc-*Bam*HI (5'- CGCGGATCCGAGGTCCTCCTCGGAGATGAGC TTCTGCTCCATGTTGGGCGAGTTTACTAATG GAAAAAG), cut with *Bgl* II and *Bam* HI and inserted into the *Bam* HI site, obliterating its 5' end, generating pORA-KUT-pACT. *PKC1* and *Cn SP1* constituent expression vectors were generated by inserting the coding region after the actin promoter (including the *c-myc* tag in the *Cn SP1* insert). *PKC1* coding region was amplified using primers PKC 1S *Bam* HI (5'- CGGGATCCATGGTGCCTG GATATCTGCCA) and PKC 3784A *Nhe*I (5'- CTAGCTAGCCTAGGCTTGTGCTGC AGCCCA). *Cn SP1* coding region was amplified using primers Crz1-1S-*Bam*HI (5'- CGGGATCCATGGCAGATCCAGCCTCAC) and Crz1 A3695 *Nhe*I (5'- CTAGCTAGCTTAATCCTCTTCACTCGTTTCAC TC). Inserts were cut with *Bam*HI and *Nhe*I and

ligated into the corresponding restriction sites in pORA-KUT-pACT, generating pORA-KUT-pACT-Cn SP1 and pORA-KUT-pACT-PKC1). A *C. neoformans*-codon adjusted GFP fragment was amplified from a previously constructed plasmid (24) by using primers GFP 1S *Bgl*II (5'-GGAAGATCTATGTCCAAGGGTGAGGAGCTC) and GFP 741A *Bam*HI (5'-CGGGATCCCTCGGCGGCGGCGG). The insert was cut with *Bam*HI and *Bgl*II and inserted in the *Bam*HI of pORA-KUT-pACT-Cn SP1, positioning the GFP on the 5' end of the coding region, generating pORA-KUT-pACT-GFP-Cn SP1. The vectors were linearized with I-Sce I and transformed by electroporation as previously described (24) as follows: pORA-KUT-pACT-PKC1 into Cn *sp1Δ* (Cn *sp1Δ*:pACT-PKC1); pORA-KUT-pACT-Cn SP1 (including the c-myc tag) into Cn *sp1Δ*, *cnalΔ* and *pkc1Δ* (Cn *sp1Δ*:pACT-Cn SP1, *cnalΔ*:pACT-Cn SP1 and *pkc1Δ*:pACT-Cn SP1, respectively); and pORA-KUT-pACT-GFP-Cn SP1 into Cn *sp1Δ* (Cn *sp1Δ*:GFP-Cn SP1).

Transformants were selected on hygromycin B and verified by sequencing. Constituent expression was tested by qRT-PCR and by western blot. Functionality of the *c-myc*-tagged Cn SP1 was verified by reversal of the Cn *sp1Δ* mutant cell-wall defects (Fig. 4).

Cell wall integrity assays-Strains were grown on YPD plus 1M sorbitol plates for 2 days at 30°C. Then, they were suspended in PBS to an OD₆₀₀ of 0.1 and underwent fivefold serial dilutions in PBS. 10 µl of each dilution was spotted on YPD; YPD + 1 M Sorbitol in 30°C and 37°C; YPD + 1 M sorbitol with the following- 0.5 mg/ml calcofluor white (Fluorescent Brightener 28, Sigma), 0.5% Congo red (Sigma), 0.01% SDS, 200 mM CaCl₂, 50 mM LiCl₂, 100 µM EDTA and 1 mM NaNO₂. Plates were incubated for 2 days at 30°C.

Caspofungin susceptibility testing- Due to the extreme fastidiousness of the *pkc1Δ* strain, we were not able to test MICs with standard broth microdilution techniques, and hence we designed a specialized agar dilution assay. Cells were grown as described above and were suspended in PBS to an OD₆₀₀ of 0.132. Cell suspensions were diluted 1:222 and 20 µl of each strain were spotted on YPD + 1 M sorbitol agar plates with caspofungin concentrations from 0.25 to 16 mg/L, including a no-drug control plate. Plates were observed for 48 hours and the MIC was determined at the point of visible growth.

Virulence factor expression and virulence studies

For measuring capsule formation under non-inducing condition, cells were grown overnight on YPD + sorbitol media and stained with India ink and observed under microscopy. Laccase activity was assessed as previously described (25). Virulence studies were conducted according to a protocol using a previously-described mouse meningoencephalitis model, with 5 mice in each group (19). Animal studies were approved by the University of Illinois at Chicago Animal Care Committee.

Microarray experiments-Cn Sp1 comparative screening by a *C. neoformans* glass microarray (Fig. 1): For the comparative transcriptional profile experiment, H99, Cn *sp1Δ*, *pkc1Δ*, *cnalΔ*, *pkalΔ*, *ssa1Δ*, *vad1Δ*, *ste12Δ*, and *bck1Δ* strains were grown over-night in YPD (with 1M Sorbitol in *pkc1Δ*) in 30°C shaker incubator to a mid-log phase and then induced by glucose starvation for 1 hour. RNA was extracted and purified, cDNA prepared, labeled and hybridized to an H99 glass microarray slides, scanned and analyzed as previously described (26-27). Feature signal was corrected for local background. Significance of signal was calculated as the two-tailed p-value of a z-test for all replicate features, using the standard deviation of all measured features on the array. P-values were corrected for False Discovery Rate (FDR) using the Benjamini-Hochberg method (28). Clustering of signal intensities were then performed in "Expression profiler" (EPCLUST website) with correlation measure-based distance and average linkage.

qRT-PCR experiments-*C. neoformans* strains were grown to a mid-log phase prior to induction. RNA was extracted before and following induction and treated with RNase-Free DNase Set (Qiagen). 5µg of total RNA were used for cDNA generation using Invitrogen SuperScript® II reverse transcriptase and oligo-dT primers in a 30 µl reaction mix. cDNA (1 µl) was used as a template for real time reactions containing primer sets and iQ™ SYBR® Green Supermix (Bio-Rad). The following primers were used in the epistasis studies: Cn SP1- Crz1 qRT2939S (5'-GTTGTCCCAA GCTATCGTCG) and Crz1 qRT3055A (5'-GACGAGCAA ACTTCTTCCCACA); PKC1-PKC cDNA 2225S (5'-CCAACAACAAGT GACGCAGAG) and PKC RT 2300A (5'-TTACCCTTACCCAG CACTGCTAA); ACT1- Actin qRT 1200S (5'-

ATGTACAATGGTATTGCCGACCGTA TG) and Actin qRT 1455A (5'-GCT CTTCGCGATCCACAT CTG) (microarray validation studies primers not shown). qPCR data was analyzed with Bio-Rad iQ5 software and results are presented either as relative expression (Δ Ct) with *ACT1* as control (epistasis studies) (29) or as normalized expression ($\Delta\Delta$ Ct) for the microarray validation studies.

Immunoprecipitation and Western Blotting-Cultures were grown overnight in YPD or in YPD containing 1 M sorbitol (150 ml) for the *pkc1Δ* strain at 30°C with shaking to mid-log phase and then induced with either 10 μg/ml calcofluor white, NaNO₂ 1mM or glucose starvation for 1h. Cells were lysed using glass-beads with phenylmethylsulfonyl fluoride (final concentration of ~1mM) and Halt® Protease and Phosphatase Inhibitor Cocktail (Pierce) and eluted with the IP Lysis/Wash buffer taken from the Pierce® Classic IP Kit (Pierce). The protein extract was adjusted to a final concentration of 1 mg/ml (2 mg/ml was used for *pkc1Δ*: pACT-Cn Sp1). 700 μl of protein extract were mixed with 5 μl of Monoclonal Anti-*c-myc* antibody produced in mouse (Sigma-Aldrich) and were incubated with rotation in 4°C for 4h. Immunoprecipitation was then carried out with the Pierce® Classic IP Kit following the manufacturer's instructions. From a final eluents' volume of 50 μl of immunoprecipitated Cn Sp1, 30 μl were loaded for the anti- phosphorylated Cn Sp1 experiment and 20 μl were run as loading control, using 7.5% SDS-PAGE. Gels were transferred overnight to a PVDF membrane, and blocked with Invitrogen's Membrane Blocking Solution. Primary antibody blot was done with either the Invitrogen Phosphoprotein Antibody Sampler Pack at a final concentration of each antibody (anti- phosphorylated serine, threonine and tyrosine) of 1 μg/ml to detect phosphorylated residues on Cn Sp1 or the anti *c-myc* antibody (1:1000) to detect total *c-myc* tagged Cn Sp1. Secondary antibody blot was done with Pierce anti Rabbit HRP diluted 1:3000 and Pierce anti Mouse HRP diluted 1:5000 (phosphorylated Cn Sp1 experiment) or Pierce anti Mouse HRP diluted 1:2500 (total Cn Sp1 experiment). Signal detection was done with the Pierce SuperSignal according to the manufacturer's directions.

Chromatin immunoprecipitation (ChIP)-ChIP was performed as previously described (30) with the following modifications. Following induction, formaldehyde was added to a final concentration of 1% and incubation was continued at room

temperature for 30 min. Cross-linking was quenched with glycine (8.5 ml of 2.5M to ~160 ml culture) at room temperature for 5 minutes. Cells were harvested, washed 3 times in cold PBS and lysed with glass beads beating. Cell extract was sonicated to produce an average size of ~750 b.p. The extract was centrifuged and supernatant was mixed with either 5 μl of anti *c-myc* or mouse IgG1 as an isotype control. Immunoprecipitation was performed as described above, except elution that was done with several washes of elution buffer (50 mM Tris-HCl pH8.0, 10 mM EDTA, 1% SDS), up to a total volume of 300 μl. DNA enrichment of promoter regions in the ChIP eluent was assayed by qPCR as described above, with the following primers: *ACT1* genomic region was used as control with primers Actin RT 739S (5'- ACCACTTCTGCCGAGCGAGA) and Actin RT 945A (5'- GAGACCAAGG AGAGAAGGCTGG); Malate dehydrogenase promoter region at -170 to 0 b.p. from ORF with primers pMDH 1396S (5'- CGAGTCGTAAACAACAGAA TGGTC) and pMDH 1576A (5'- TACGGGTCATT CTGGGCTGG); 1,4- α -glucan-branching enzyme promoter region at -291 to -40 from ORF with primers α -glucan prom RT 1009S (5'- CGAAAGCGGC AAGTCAG GTG) and α -glucan prom RT 1063A (5'- GACTGAAG ACGAGAAATGAGAAGGGA); and *HSP12* promoter region at -300 to -210 from ORF with primers *HSP12* promoter RT S (5'- GCAGCAACACAAGCAGCA A) and *HSP12* promoter RT A (5'- CGGCAAGAACCAGCAACAG). Promoter occupancy by Cn Sp1 was expressed as a ratio of the target promoter signal immunoprecipitated to the *c-myc* antibody vs. the isotype control; the ratio in the *ACT1* genomic region was used as a control.

Fluorescent microscopy of GFP-tagged Cn Sp1-

Cells were grown over-night to a mid-log phase prior to induction as described above. At each time point, slides were prepared with diamidino-2-phenylindole (DAPI) and observed under fluorescent microscopy as described (31). Triplicates of 100 cells each were observed for nuclear localization and expressed as mean \pm SD.

Statistics-Statistical significance of mouse survival times was assessed by Kruskal-Wallis analysis (ANOVA on Ranks). Statistical analysis was conducted using GraphPad Prism software, version 4.03.

RESULTS

CNAG_00156 is not a functional homolog of yeast CRZ1 despite sequence similarity. We identified *CNAG_00156* as a potential homolog of the *S. cerevisiae* calcineurin-responsive transcription factor (Crz1), based on highest similarity (58.7%) to the ascomycete factor. However, during our study, this hypothesis appeared unlikely, based on three lines of evidence: 1) Lack of restoration of temperature-dependent or cell-wall defective phenotypes after over-expression of *CNAG_00156* in *cnal1Δ* (*cnal1Δ*:pACT-Cn *SP1*) (Fig. S1A); 2) lack of a calcineurin-dependent size shift of the *CNAG_00156* protein on SDS-PAGE gel suggesting a lack of calcineurin-dependent post-translational modifications (Fig. S1C) (32-33); 3) lack of calcium-dependent nuclear translocation of a GFP-tagged *CNAG_00156* (Fig. S1D) previously demonstrated with Crz1 homologs (32-33).

*Transcriptional profiling reveals that *cnag_00156Δ* and *pkc1Δ* mutant strains share similar transcriptional profiles under starvation conditions.* To elucidate the potential cellular pathway related to *CNAG_00156*, we compared the transcriptional profile of *cnag_00156Δ* with knockout mutants of genes involved in laccase production- *pka1Δ*, *pkc1Δ*, *ssa1Δ* and *vad1Δ*, as well as genes related to pathways with a known C-terminal Zinc-finger transcription factor in *S. cerevisiae*: *cbk1Δ* (RAM pathway) and *cnal1Δ*. An *ssa1Δ* mutant in an H99 background was constructed for these studies and is described in Supplemental Methods (Fig. S8). The *ste12Δ* mutant, which has wild type virulence and laccase expression in the H99 background (34) was chosen as an outgroup control. Since nutrient starvation is a condition required for induction of numerous virulence-associated cellular programs such as autophagy (20) and laccase expression (35), glucose starvation conditions were chosen for the strain comparisons.

Compared with the other mutants, the *pkc1Δ* strain exhibited the most similar transcriptional profile to *cnag_00156Δ* (Figs. 1A-B; Fig. S2), with 48 shared downregulated genes (out of 208 and 194 downregulated genes in *cnag_00156Δ* and *pkc1Δ*, respectively), supporting a possible common pathway. Validation of sample genes from the microarray experiment was performed by northern blot (Fig. S4) and qRT-PCR studies (Fig. S5) and will be described in further detail later.

*CNAG_00156 shares homology to C-terminal Zn finger transcription factors in *S. cerevisiae* and *H. sapiens*.* Comparison of the full-length putative amino acid sequence of *CNAG_00156* with other known C-terminal Zinc-finger TFs of *S. cerevisiae* failed to identify homologous yeast Zn finger proteins (Fig. 1C, blue frame) known to be related to Pkc1. Indeed, the known *PKC1*-related TFs in *S. cerevisiae*, Rlm1 and Swi4, are not C-terminal Zinc-finger proteins. In contrast, metazoans, represented by mammalian (*H. sapiens*) cells (Fig. 1C, tan frame) express several *CNAG_00156* homologs with homology to the Sp TF family (58.7% and 54.5% similarity with Crz1 and Sp1, respectively). Interestingly, within the Sp TF family, Sp1 and Sp3 are known to be regulated by Pkc1 (36-37). Based on this homology, we decided to designate *CNAG_00156* as *C. neoformans SP1* (Cn *SP1*). *Structural analysis of Cn Sp1, H. sapiens Sp1 and S. cerevisiae Crz1.* To better understand the structural relationship between Cn Sp1 and metazoan Sp1, we compared the Zn finger elements of Cn Sp1 to that of the *S. cerevisiae* Crz1 and the archetype *H. sapiens* Sp1 since this region of the protein is the most highly conserved across species and is an important functional motif. SMART analysis (38) showed that the distribution of the C-terminal zinc finger domains were of similar pattern in both Cn Sp1 and *H. sapiens* Sp1 (Fig. 2a) with three domains in Cn Sp1 (944-968, 974-1001 and 1007-1034) and *H. sapiens* Sp1 (626-650, 656-680 and 686-708) and only two domains (569-591 and 597-619) in Crz1 from *S. cerevisiae*. This is an important divergence as the Zn finger domain is the principal DNA-binding element within these classes of transcription factors (39-40).

Phylogenetic analysis of homologous C-terminal Zn finger domains across selected fungi and metazoans revealed further sequence divergence between the basidiomycete factor and those of ascomycetes such as Crz1 (Fig. 2B, S3A). Interestingly, the first Zn finger domain of basidiomycete fungi such as *C. neoformans* appears to cluster best with metazoans rather than ascomycete yeast such as *S. cerevisiae*, although the relationship was weakly supported due to the short sequences of the motif. In contrast, the second Zn finger motif appears to follow classic evolutionary relationships with basidiomycete fungi clustering with the ascomycete motif. The third Zn finger motif of *C. neoformans* fulfills the protein family

definition of a Zn finger motif (C-X(1-5)-C-X12 -H-X(3-6) – [H/C] (41) similar to the metazoan Zn finger motifs (Fig. S3B). However, a previously undescribed motif bearing a resemblance to Zn-finger domains was also found in the *S. cerevisiae* Crz1 factor. A 9 amino-acid insertion between the first two cysteine residues results in its failure to be classified as a canonical Zn finger motif. It is not known whether this region in *S. cerevisiae* plays a role in DNA binding although recent studies suggest the importance of three Zn motifs in DNA binding (42). Nevertheless, these studies demonstrate an evolutionary divergence between the cryptococcal Sp1 and the ascomycete Crz1.

A Cn sp1Δ mutant shares virulence factor and cell-wall defects with a cryptococcal pkc1Δ mutant. To establish a correlation between Cn SP1 and the PKC1 pathways, we compared phenotypic features of the two mutants which showed a number of qualitative similarities. Both mutants had similar glossy-shiny colony morphologies on non-inducing conditions, due to subtly increased capsule production as previously demonstrated by the same method for the *pkc1Δ* strain (16) (Fig. S6). India ink microscopy (Fig. 3B) of the two strains under the same conditions also demonstrated a shared increased capsule production in both, although the effect from the Cn *sp1Δ* mutation was more pronounced. Both mutants also shared decreased laccase production (Fig. 3C) which was more profound in the *pkc1Δ* mutant. Importantly, Cn *sp1Δ* exhibited attenuated virulence in a mouse model, showing the capacity for Cn SP1 to mediate PKC1-mediated effects on virulence (Fig. 3D). While not explicitly tested for virulence in previous reports (16) the cryptococcal *pkc1Δ* mutant would be expected to be avirulent, based on its inability to grow at 37° C. Both mutants also exhibited cell wall/membrane dysfunction, manifested by sensitivity to cations and cell-wall inhibitors, as well as to the nitrosative agent NaNO₂ (Fig. 4 and Table 1). We also tested susceptibility of the strains to the pharmaceutical cell-wall agent caspofungin which showed that the Cn *sp1Δ* mutant displayed an intermediate sensitivity by minimum inhibitory sensitivity (MIC) between wt and the *pkc1Δ* strains (wt, Cn *sp1Δ*:: Cn SP1 and *pkc1Δ*::PKC1: 8 mg/ml; Cn *sp1Δ*: 4 mg/ml and *pkc1Δ*: 0.25 mg/ml) suggesting a role for Cn SP1 in resistance to this cell wall-active antifungal agent. In summary, cell wall dysfunction was more profound in the *pkc1Δ* strain

in comparison to the Cn *sp1Δ* mutant, suggesting that Cn Sp1 may partially mediate a subset of PKC1-dependent phenotypes. However, unlike the *pkc1Δ* strain, Cn *sp1Δ* did not have a growth restriction at 37°C with sorbitol or 30°C in the absence of sorbitol (Figs. 3A, 4), suggesting no contribution of Cn Sp1 to these PKC1-dependent phenotypes.

Overexpression of Cn SP1 partially restores cell wall integrity defects in a cryptococcal pkc1Δ mutant strain. To examine epistatic relationships between PKC1 and Cn SP1, plasmids expressing each gene under the actin promoter were constructed and transformed into the other respective mutant and overexpression confirmed by qPCR [normalized expression (+/- SD): Cn SP1 expression in *pkc1Δ*:pACT-Cn SP1/*pkc1Δ*: 2.5 (+/- 0.5); PKC1 expression in Cn *sp1Δ*:: pACT-PKC1/Cn *sp1Δ*: 4.3 (+/- 1.6)]. Lack of PKC1 expression in the *pkc1Δ*::pACT-Cn SP1 strain was also confirmed by reverse-transcription PCR (data not shown). The *pkc1Δ*::pACT-Cn SP1 strain demonstrated partially restored cell wall integrity (Fig. 4, Table 1) in YPD without sorbitol, as well as in YPD/sorbitol containing calcofluor-white, SDS, CaCl₂, LiCl₂ and NaNO₂ (Fig. 4). SP1 overexpression in the *pkc1Δ* mutant also partially restored the "dry" appearance of plated colonies (Fig. S6), and successfully restored the wt repressed capsule phenotype (Fig. 3B). Features that were not restored in the Cn SP1-overexpressing strain compared with the *pkc1Δ* strain were growth in 37°C and in YPD/sorbitol with Congo red (Fig. 4), laccase expression (Fig. 2), and a reduced caspofungin MIC which remained at 0.25. In contrast, overexpression of PKC1 in the Cn *sp1Δ* mutant did not alter any growth, capsule or cell wall phenotypes including caspofungin sensitivity. These results support the hypothesis that Cn SP1 acts downstream to PKC1, regulating a sub-population of cell-wall integrity functions.

Regulation of Cn SP1. We next sought to study the effect of glucose starvation on Cn Sp1 since a recently described role for autophagy suggests that nutrient deprivation plays an important role during cryptococcal infection (20) and laccase is known to be derepressed in the absence of glucose (43). In addition, because of the possible role of Cn Sp1 in the Pkc1 pathway, we studied conditions shown previously to be Pkc1 dependent: calcofluor-white (CFW) and NaNO₂ (16). As shown in Fig. 5A, Cn SP1 transcription is induced under glucose starvation and was found to be dependent on an intact PKC1

locus. During induction with calcofluor white and NaNO_2 , Cn *SP1* transcript levels remained steady or slightly reduced (Figs. 5B and C, respectively) and were higher in the *pkc1Δ* compare to wt. Secondly, since *PKC1* is known to regulate the activity of transcription factors by phosphorylation, we analyzed for this by immunoprecipitating an N-terminal *c-myc*-tagged Cn Sp1 in a Cn *sp1Δ* background (Cn *sp1Δ*:pACT-Cn *SP1*) (Fig. 5D), followed by western blotting using an anti-phosphoserine/threonine/tyrosine antibody (Fig. 5E). Interestingly, the Pkc1-inducing conditions CFW and NaNO_2 , led to an increase in the phosphorylation of Cn Sp1 whereas there was no increase in phosphorylation under glucose starvation, suggesting complementary transcriptional and post-translational regulation of Cn Sp1 by Pkc1. Next, we studied the effect of these three conditions on the localization of GFP-Cn Sp1. As shown in Fig. 5F, a subset of the Cn Sp1 protein fraction is constitutively present in the nucleus, even under mid-log growth conditions in YPD. However nuclear fractional localization of Cn Sp1 was increased during induction with CFW and NaNO_2 but not after glucose starvation (Fig. 5. F-G) again suggesting both transcriptional and post-translational regulation by Pkc1. Both mechanisms would be expected to result in total nuclear quota of the Cn Sp1 protein under all three inducing conditions by this combination of mechanisms, resulting in successful Pkc1-dependent signaling through Cn Sp1.

Cn SP1 and PKC1 mediate a similar transcriptional response to glucose starvation.

We next conducted additional whole-genome epistatic experiments of Cn *SP1* and *PKC1* under starvation using microarray analysis (see ‘Experimental Procedures’). Fig. 6a shows a Y vs. X plot whereby Y describes transcript level changes of the Cn *sp1Δ* mutant compared to that of the wild type under starvation conditions; X describes transcriptional differences between the *pkc1Δ* mutant and wild type, all under starvation conditions. The finding of a significant correlation in both direction and expression levels between the Cn *sp1Δ* and the *pkc1Δ* mutants (slope of $y = \log_2(\text{Cn } sp1\Delta / \text{wt})$ vs. $\log_2(\text{pkc1}\Delta / \text{wt})$: 0.5907 ± 0.01 ; $p < 0.0001$) suggests a genetic relationship between the two genes, whereby genes down regulated in the first mutant also tended to be downregulated in the second. Using these plots we first identified genes

that were significantly downregulated in both the *pkc1Δ* and Cn *sp1Δ* strains with a False Discovery Rate (FDR) of <0.05 (Fig. 6A, red + green dots). From these, we selected the genes that were downregulated by at least 2-fold (Fig. 6A, green dots). Of the 6970-genes tested in the microarray, 163 met both criteria (Table 2). Consistent with these results, over expression of Cn *SP1* in the *pkc1Δ* mutant (*pkc1Δ*:pACT-Cn *SP1*) restored expression of a large majority of these genes, either completely or partially (>2 fold compared to *pkc1Δ*) in 102 genes (Fig. 6C; Table 2). Analysis of the entire transcriptome also showed a significant restoration of *PKC1*-dependent gene expression levels after Cn *SP1* overexpression as evidenced by a reversal of the slope of Fig. 6B vs. that of Fig. 6A and a regression having a significant negative slope [slope of $y = \log_2(\text{pkc1}\Delta:\text{pACT-Cn } SP1 / \text{pkc1}\Delta)$ vs. $\log_2(\text{pkc1}\Delta / \text{wt})$: -0.495 ± 0.005 ; $p < 0.0001$]. Interestingly, careful comparison of the transcriptional profiles of the *sp1Δ* strain (Fig. 6A) to that of the *SP1* overexpressor strain (Fig. 6C) identified numerous black-labeled genes that were scored as non-significant but showed significant upregulation after *SP1* overexpression. One such gene, *HSP12* was confirmed by northern blot analysis to show reduced transcription in the *sp1Δ* mutant that was restored after *SP1* overexpression (Fig. S4a). This reflects the relative conservative nature of the false discovery methodology commonly used for determining significance in transcriptional differences and shows the utility of whole genome epistatic studies in improving the efficiency of gene discovery in microarray experiments. Hsp12 has been recently found to display cAMP-dependent gene transcription in fungal pathogens *Candida albicans* as well as *C. neoformans* and was found in the latter to have a role in polyene antifungal drug susceptibility (43, 44). Interestingly, the majority of the population of Cn *SP1/PKC1* dependent genes (151/163) were also induced in the wt strain during transition from mid-log phase growth to starvation conditions (Fig. 6C) suggesting an important role for the *PKC1*-Cn *SP1* pathway during nutrient stress.

Table 2 details genes that were downregulated >2 fold with an $\text{FDR} < 0.05$ in both *pkc1Δ* and Cn *sp1Δ* following glucose starvation. Functionally, these genes include those involved in carbohydrate metabolism, membrane transporters and channels, and general stress response (see

overview, Fig. 6D). Genes involved in several virulence pathways were identified including the *NTH1* gene involved in trehalose metabolism (45) and the allergen 1 gene involved in mucoid switch variants of *C. neoformans* (46). We validated the results presented in Table 2 and Fig. 6 by confirmation of a subset of genes by either northern blot (Fig. S4a) or qRT-PCR (Fig. S4b). We also confirmed several additional genes of interest that were found to be downregulated in the mutants but had not met the statistical criteria similar to *HSP12* described above (Fig. S4). For example, expression of 1,3- β glucan synthase, a target of the anti-fungal caspofungin (47) and a critical cell-wall synthesis enzyme in *C. neoformans* (48), is increased following starvation in wt, but decreased in *pkc1 Δ* and Cn *sp1 Δ* . Wt expression is partially restored in the *pkc1 Δ* :pACT-Cn *SP1* strain. This reduction may partially explain the increased susceptibility to caspofungin of both the Cn *sp1 Δ* and the *pkc1 Δ* mutants. However, lack of restoration of caspofungin resistance in the *pkc1 Δ* mutant by Cn *Sp1* described above supports a role for additional genes in this unique cryptococcal resistance besides 1,3- β glucan synthase expression as suggested recently (49). The transcription of laccase was also reduced in the Cn *sp1 Δ* but not in *pkc1 Δ* (Fig. S4), despite reduced enzymatic activity in both (Fig. 3C), suggesting a complexity of regulation of this gene involving both transcriptional and post-transcriptional mechanisms.

Cn Sp1 binds to promoter regions of Cn Sp1/Pkc1-dependent genes. Chromatin immunoprecipitation (ChIP) was performed using the Cn *sp1 Δ* :pACT-Cn *SP1* strain which expresses Cn *Sp1* as a fusion with a *c-myc* affinity tag (see 'Experimental Procedures'). Immunoprecipitation was performed using either an anti *c-myc* monoclonal Ab or a mouse IgG1 isotype control antibody and promoter occupancy quantified using a qPCR assay. Promoter occupancy was expressed as a ratio of the target promoter signal immunoprecipitated by the *c-myc* antibody vs. the isotype control. Following glucose starvation, promoters of *HSP12* and malate dehydrogenase (MDH) showed increased promoter occupancy ratios of 230 \pm 5.9, and 295.4 \pm 37.4, respectively, whereas in mid-log phase cells Cn *Sp1* occupancy was increased for the *MDH* but not the *HSP12* promoters (29.7 \pm 4.5 vs. 0.61 \pm 0.09, respectively). In contrast, DNA encoding the unrelated actin gene showed no enrichment after *c-myc*

immunoprecipitation (data not shown). Furthermore, during starvation, the ratio of 1,4- α -glucan branching enzyme promoter to actin was 1.4 \pm 0.34, and target gene signals were undetectable in mid-log phase cells, suggesting that this gene is not a direct target of Cn *Sp1*.

DISCUSSION

Previous work demonstrated that cryptococcal virulence and laccase expression is dependent on activation of the protein kinase C pathway by diacylglycerol (50, 51). A multiple component pathway emanates from *PKC1*: one mediated through the Map kinase signaling members, Bck1, Mkk2 and Mpk1 responsible for growth at high temperature and cell wall integrity and an additional unknown pathway(s) responsible for laccase expression, capsule regulation and nitrosative stress (17). The present work confirms the existence of an additional parallel pathway and identifies a novel Pkc1-dependent C-terminal Zn finger transcription factor in fungi (Fig. 7). The reliance of the TF on Pkc1 was suggested by a screen using a microarray-based transcriptional comparison to known signal transduction mutants. An association with Pkc1 was then confirmed by a series of biochemical and epistatic experiments. The cryptococcal transcription factor was named Cn *Sp1* since it is homologous to the Sp1/KLF transcription factor family within metazoans that, like Cn *Sp1*, contains three C-terminal Cys2His2-type Zn finger motifs.

Interestingly, Cn *Sp1* also bears sequence similarity to a group of ascomycete C-terminal transcription factors with closest homology, by a simple BLAST search, to the calcineurin-responsive Zn finger protein, Crz1, but these typically contain only two canonical C-terminal Zn finger motifs (Fig. 2). Calcineurin-dependent signaling is important in a number of cellular processes in *C. neoformans* including growth at elevated temperature, virulence and sexual development. Expression of the virulence factor laccase also appears to be dependent on calcineurin as evidenced by a role in calcium-dependent expression mediated by the transcriptional co-activator, Ssa1 and Ssa1's dependence on Crz1 in *S. cerevisiae* (52). However, our studies showed that mutants of the cryptococcal Cn *Sp1* did not share phenotypes with that of the calcineurin mutant *cna1 Δ* , did not display calcineurin-dependent size shifts on a SDS-PAGE

gel, and did not display calcium-dependent nuclear localization, typical of the calcineurin-dependent ascomycete factor. This led us to screen for other potential signal transduction pathways using a microarray comparison screening approach.

Analysis of the C-terminal Zn finger motifs of Cn Sp1 allowed an evolutionary comparison of similar proteins within both fungi and metazoans as this region is more highly conserved and are an important functional signature of both the Crz1 and Sp family of proteins (39-40). These studies demonstrated a complex evolutionary divergence of the cryptococcal TF from that of ascomycetes such as *S. cerevisiae*. For example, while the second cryptococcal Zn finger motif shares closest homology to the second of two Zn finger motifs of the ascomycete Crz1, the first displays closer similarity to that of the metazoan and plant Sp/KLF homologs. Examination of a third cryptococcal Zn finger motif shows that it superficially displays homology to a non-canonical Zn finger-like motif within the ascomycete factors that has not been described previously. Excluding the ascomycete site would again place the cryptococcal canonical Zn finger site closest to the metazoan canonical Zn finger motifs. However, retention of the cysteine and histidine-containing ascomycete sequences during evolution suggests that this third non-canonical Zn finger-like motif may have retained function. Since recent structural studies suggest a role for the third Zn finger motifs in determining DNA sequence specificity and binding affinity, this divergent ascomycete motif could play a role in differentiating the DNA sequences recognized between the mammalian and ascomycete TFs as described previously (40, 52). Interestingly, analysis of promoter sequences from the *HSP12* and *MDH* genes that showed Cn Sp1 promoter occupancy by chromatin immunoprecipitation contain consensus Sp1 binding sites (*Hsp12*: ⁴⁹⁰CCGCCC; *MDH*: ⁵⁹CCGCCC) but do not contain consensus Crz1 binding sites, again suggesting greater similarity to the metazoan TF. However, more detailed promoter dissection studies are required to confirm these findings. In addition, examination of the *C. neoformans* annotated database (Broad Institute website) identified two C-terminal Zn finger proteins (*CNAG_00039* and *CNAG_01014*) that contained the requisite two Zn finger motifs of Crz1 but these did not share strong homology to the Crz1 protein either by BLAST or Clustal-W algorithms. This

suggests an evolutionary loss of the primordial Crz1 gene product function in *C. neoformans*. Indeed, previous attempts to identify a Crz1 homolog in *C. neoformans* by a number of methods including a multi-copy suppressor screen of a cryptococcal calcineurin mutant failed to identify functional homologs of Crz1 in *C. neoformans* (27).

Interestingly, the Sp/KLF class of metazoan transcription factors is regulated by a variety of signal pathways including protein-kinase homologs *PKCζ* which have been best studied in mammalian systems (40). These C-terminal transcription factors are also regulated by phosphorylation, similar to the cryptococcal factor. The metazoan TF's also act as coactivators of multiple pathways including Ras and phosphatidyl 3-kinase pathways, suggesting interesting precedents to examine for Cn Sp1 in the future. However, it is important to be cautious in extrapolating functions to the cryptococcal Sp1, based on the distant phylogenetic relationships involved. Additional structural studies will be needed to differentiate Cn Sp1 from the metazoan factors.

While it is difficult to make precise comparisons of functionality, it appears that the evolutionary structural drift of the fungal C-terminal Zn finger protein from Crz1 to Cn Sp1 also resulted in changes in the types of cellular functions regulated by this factor as compared to that reported previously for Crz1 from *S. cerevisiae* (39). For example, while a variety of cell wall synthetic functions are regulated by both Crz1 (chitin synthase type I, 1,3 b-glucan synthesis regulator *RHO1*) and Cn Sp1 (1,3-β glucan synthase), Cn Sp1 appears to have picked up additional target functions in carbohydrate metabolism including trehalose regulation and amino acid metabolism (such as the Rds1 protein, homologs of which are involved in ubiquitin-binding degradative functions, 53). In addition, expression of degradative target genes of *crz1* such as carboxypeptidase and Atg5, the latter involved in autophagy induction (54), appears to have been lost in the evolution towards a *pkc1*-dependent factor. Such changes in the regulatory landscape may have optimized relationships between environmental signals to cellular outputs that resulted in its evolution to a mammalian pathogen. Indeed, the cryptococcal Sp factor was found to mediate several important *Pkc1*-dependent phenotypes peculiar to its role as a pathogen including capsule regulation and resistance to nitrosative stress. Importantly, Cn Sp1

was required for wild-type virulence in a mouse model. However, while the Cn *SP1* mutant was defective in laccase expression, epistatic studies did not show restoration of the *pkc1* laccase defect after Cn *SP1* overexpression, suggesting a role for additional pathway(s) mediating Pkc1-dependent laccase expression. Interestingly, our microarray epistatic transcriptional studies suggest that a preponderance of Pkc1-mediated transcription is dependent on Cn Sp1 signaling under glucose depletion conditions. However, these data should not be interpreted as implicating Cn Sp1 in all Pkc1-mediated transcription as cross talk and the role of the parallel MAPK pathway may lead to less reliance on Cn Sp1 under other Pkc1-associated conditions such as oxidative or nitrosative stress. Interestingly, dependence of some genes such as malate dehydrogenase showed strong reliance on both Pkc1 and Cn Sp1 by northern analysis, whereas glucan synthase showed less dependence, suggesting such a role for multiple interacting signals communicating with Cn Sp1. Examination of the microarray epistatic experiments appear to bear this out with a large variation in both *PKC1* and Cn *SP1*-

dependent expression levels across the *C. neoformans* transcriptome. Such data show the advantage of a consideration of the whole genome in determining the regulatory impact of components of a signal transduction pathway. Induction of the glucose starvation response by Pkc1/Cn Sp1 may be particularly important in cryptococcal infections where nutrient-deficiency encountered in host macrophages and brain is suggested by a role for autophagy during pathogenesis (20). Nutrient stress, in combination with host oxidative and temperature stress are environmental components against which the fungus must compete for successful infection. The ability of the organism to induce transcriptional programs during nutrient limitation such as that mediated by Pkc1-Cn Sp1 modeled here during starvation may be a key component in niches leading to low metabolic states such as during latent infection, demonstrated in recent clinical studies showing long periods of time within the host between initial infection and manifestation of disease during HIV-mediated immune suppression (55).

REFERENCES

1. Bichile, L., Gokhale, Y., Sridhar, V., and Gill, N. (2001) *J Assoc Physicians India* **49**, 377–378
2. Casadevall, A., and Perfect, J.R. (1998) *Cryptococcus neoformans*. ASM Press. Washington, D.C., USA. 541
3. French, N., Gray, K., Watera, C., Nakiyingi, J., Lugada, E., Moore, M., Lalloo, D., Whitworth, J.A., and Gilks, C.F. (2002) *AIDS*. **16**(7), 1031–1038
4. Park, B.J., Wannemuehler, K.A., Marston, B.J., Govender, N., Pappas, P.G., and Chiller, T.M. (2009) *AIDS* **23**(4), 525–530
5. Odom, A., Muir, S., Lim, E., Toffaletti, D.L., Perfect, J., and Heitman, J. (1997) *EMBO J*. **16**(10), 2576–2589
6. Salas, S.D., Bennett, J.E., Kwon-Chung, K.J., Perfect, J.R., and Williamson, P.R. (1996) *J Exp Med* **184**(2), 377–386
7. Chang, Y.C., and Kwon-Chung, K.J. (1994) *Mol Cell Biol* **14**(7), 4912–4919
8. Chang, Y.C., Penoyer, L.A., and Kwon-Chung, K.J. (1996) *Infect Immun* **64**(6), 1977–1983
9. Chang, Y.C., and Kwon-Chung, K.J. (1998) *Infect Immun* **66**(5), 2230–2236
10. Perez, P., and Calonge, T.M. (2002) *J Biochem* **132**(4), 513–517
11. Jung, U.S., and Levin, D.E. (1999) *Mol Microbiol* **34**(5), 1049–1057
12. Jung, U.S., Sobering, A.K., Romeo, M.J., and Levin, D.E. (2002) *Mol Microbiol* **46**(3), 781–789
13. Watanabe, Y., Irie, K., and Matsumoto, K. (1995) *Mol Cell Biol* **15**(10), 5740–5749
14. Watanabe, Y., Takaesu, G., Hagiwara, M., Irie, K., and Matsumoto, K. (1997) *Mol Cell Biol* **17**(5), 2615–2623
15. Kim, K.Y., Truman, A.W., and Levin, D.E. (2008) *Mol Cell Biol* **28**(8), 2579–2589
16. Gerik, K.J., Bhimireddy, S.R., Ryerse, J.S., Specht, C.A., and Lodge, J.K. (2008) *Eukaryot Cell* **7**(10), 1685–1698

17. Gerik, K.J., Donlin, M.J., Soto, C.E., Banks, A.M., Banks, I.R., Maligie, M.A., Selitrennikoff, C.P., and Lodge, J.K. (2005) *Mol Microbiol* **58**(2), 393-408
18. Zhang, S., Hacham, M., Panepinto, J., Hu, G., Shin, S., Zhu, X., and Williamson, P.R. (2006) *Mol Micro* **62**(4) 1090-1101
19. Waterman, S.R., Hacham, M., Panepinto, J., Hu, G., Shin, S., and Williamson, P.R. (2007) *Infect Immun* **75**(2), 714-722
20. Hu, G., Hacham, M., Waterman, S.R., Panepinto, J., Shin, S., Liu, X., Gibbons, J., Valyi-Nagy, T., Obara, K., Jaffe, H.A., Ohsumi, Y., and Williamson, P.R. (2008) *J Clin Invest* **118**(3), 1186-1197
21. Cox, G.M., Toffaletti, D.L., and Perfect, J.R. (1996) *J Med Vet Mycol* **34**(6), 385-391
22. Edgar, R.C. (2004) *Nucleic Acid Res* **32**(5) 1792-1797
23. Swofford, D.L. (2003) *PAUP*. Phylogenetic Analysis Using Parsimony (*and Other Methods)*. Version 4, Sinauer Associates, Sunderland, Massachusetts
24. Liu, X., Hu, G., Panepinto, J., and Williamson, P.R. (2006). *Mol Microbiol* **61**(5), 1132-1146
25. Liu, L., Tewari, R.P., and Williamson, P.R. (1999). *Infect Immun* **67**(11), 6034-6039
26. Park, Y.D., Panepinto, J., Shin, S., Larsen, P., Giles, S., and Williamson, P.R. (2010) *J Biol Chem* **285**(45), 34746-34756
27. Kraus, P.R., Boily, M.J., Giles, S.S., Stajich, J.E., Allen, A., Cox, G.M., Dietrich, F.S., Perfect, J.R., and Heitman, J. (2004) *Eukaryot Cell* **3**(5), 1249-1260
28. Benjamini, Y., and Hochberg, Y. *Controlling the False Discovery Rate: a Practical and Powerful Approach to Multiple Testing* (1995). *J. Roy. Statistical Society* **57**, 289-300
29. Chow, E.D., Liu, O.W., O'Brien, S., and Madhani, H.D. (2007) *Curr Genet* **52**(3-4), 137-148
30. Ren, B., Robert, F., Wyrick, J.J., Aparicio, O., Jennings, E.G., Simon, I., Zeitlinger, J., Schreiber, J., Hannett, N., Kanin, E., Volkert, T.L., Wilson, C.J., Bell, S.P., and Young, R.A. (2000) *Science* **290**(5500), 2306-2309
31. Zhu, X., Gibbons, J., Garcia-Rivera, J., Casadevall, A., and Williamson, P.R. (2001) *Infect Immun* **69**(9), 5589-5596
32. Boustany, L.M., and Cyert, M.S. (2002) *Genes Dev* **16**(5), 608-619
33. Karababa, M., Valentino, E., Pardini, G., Coste, A.T., Bille, J., Sanglard, D. (2006) *Mol Microbiol* **59**(5), 1429-1451
34. Yue, C., Cavallo, L.M., Alspaugh, J.A., Wang, P., Cox, G.M., Perfect, J.R., and Heitman, J. (1999) *Genetics* **153**(4), 1601-1615
35. Williamson, P.R. (1994) *J Bacteriol* **176**(3), 656-664
36. Rafty, L.A., and Khachigian, L.M. (2001) *Nucleic Acids Res* **29**(5), 1027-1033
37. Cramer, T., Jüttner, S., Plath, T., Mergler, S., Seufferlein, T., Wang, T.C., Merchant, J., and Höcker, M. (2008) *Cell Signal* **20**(1), 60-72
38. Schultz, J., Milpetz, F., Bork, P., and Ponting, C.P. (1998) *Proc Natl Acad Sci USA* **95**(11), 5857-5864
39. Cyert, M.S. (2003) *Biochem Biophys Res Commun* **311**(4), 1143-1150
40. Wierstra, I. (2008) *Biochem Biophys Res Commun* **372**(1), 1-13
41. Klug, A., and Schwabe, J.W. (1995) *FASEB J* **9**(8), 597-604
42. Lee, J., Kim, J.S., and Seok, C. (2010) *J Phys Chem* **114**(22), 7622-7671
43. Maeng, S., Ko, YJ, Kim, GB, Jung, KW, Floyd, A., Heitman, J. and Bahn, YS, (2010) *Eukaryot Cell* **9**(3), 360-378.
44. Sheth, C.C., Mogensen, E.G., Fu, M.S., Blomfield, I.C., Muhlschlegel, F.A., (2008) *Fungal Genet Biol* **45**(7), 1075-80.
45. Ngamskulrungraj, P., Himmelreich, U., Brege, r J.A., Wilson, C., Chayakulkeeree, M., Krockenberger, M.B., Malik, R., Daniel, H.M., Toffaletti, D., Djordjevic, J.T., Mylonakis, E., Meyer, W., Perfect, J.R. (2009) *Infect Immun* **77**(10), 4584-96.
46. Jain N, Li L, Hsueh YP, Guerrero A, Heitman J, Goldman DL, Fries BC. (2009) *Infect Immun* **77**(1), 128-40.
47. Kartsonis, N.A., Nielsen, J., Dougla, s C.M. (2003) *Drug Resist Updat* **6**(4), 197-218.

48. Thompson, J.R., Douglas, C.M., Li, W., Jue, C.K., Pramanik, B., Yuan, X., Rude, T.H., Toffaletti, D.L., Perfect, J.R., Kurtz, M. (1999) *J Bacteriol* **181**(2), 444-53.
49. Maligie, M.A. and Selitrennikoff, C.P. (2005) *Antimicrob Agents Chemother* **49**(7), 2851-6.
50. Heung, L.J., Luberto, C., Plowden, A., Hannun, Y.A., and Del Poeta, M. (2004) *J Biol Chem* **279**(20), 21144-21153
51. Heung, L.J., Kaiser, A.E., Luberto, C., and Del Poeta, M. (2005) *J Biol Chem* **280**(31), 28547-28555
52. Yoshimoto, H., Saltsman, K., Gasch, A.P., Li, H.X., Ogawa, N., Botstein, D., Brown, P.O., and Cyert, M.S. (2002) *J Biol Chem* **277**(34), 31079-31088
53. Yashiroda, H., Kaida, D., Toh-e, A., Kikuchi Y. (1988) *Gene* **225**(1-2), 39-46.
54. Yang, Z., Klionsky, D.J. (2010) *Nat Cell Biol* **12**(9), 814-22.
55. Dromer, F., Mathoulin, S., Dupont, B., and Laporte, A. (1996) *Clin Infect Dis* **23**(1), 82-90

FOOTNOTES

This work was supported, in part, by United States Public Health Service Grant NIH-AI45995, AI49371. This research was also supported, in part, by the Intramural Research Program of the NIH, NIAID.

FIGURE LEGENDS

Fig 1. Transcriptional and protein sequence comparison of a C-terminal Zn finger (CNAG_00156).

A. Heatmap display of a comparative microarray experiment of *C. neoformans* strains *Cn sp1Δ* (*cnag_00156Δ*), *pkc1Δ*, *pka1Δ*, *cna1Δ*, *cbk1Δ*, *ssa1Δ*, *stel2Δ*, and *vad1Δ*. Strains were grown over-night to mid-log phase, and induced in 0% glucose media for 1 hour before RNA extraction. wt (H99) induced under the same conditions was used as reference for each mutant. A cluster analysis of genes significantly altered in mutant strains with $p < 0.0001$ are presented. *B.* Close-up figure of the cluster analysis presented in panel a. *C.* Neighbor-joining phylogenetic analysis of the Cn Sp1 (Cnag_00156) with *S. cerevisiae* (blue frame) and *H. sapiens* (tan frame) C-terminal zinc-finger transcription factors

Fig. 2. *C. neoformans* and the *H. sapiens* Sp1 share similar functional domains. *A.* The SMART-identified Zinc Finger domain pattern, showing Cn Sp1, Crz1 and *H. sapiens* Sp1 zinc finger domains (ZnF). *B.* Phylogenetic analysis of metazoan and fungal zinc finger motifs, ZnF-1-3 of *C. neoformans*. Parsimonious trees were constructed using the heuristic parsimony algorithm of PAUP 4b10 as described in Experimental Methods. Clades consisting of major taxonomic groups were collapsed when possible. Bootstrap support percentages greater than 70% are shown above the branches.

Fig. 3. *Cn sp1Δ* and *pkc1Δ* have altered virulence factors. *A.* wt (H99), *Cn sp1Δ* and *Cn sp1Δ::Cn SPI* strains were grown on YPD media and suspended in PBS to OD₆₀₀ of 0.1. Five 5-fold dilutions of each strain were spotted on YPD agar plates, incubated in 37°C and observed for 48 hours. *B.* wt, *Cn sp1Δ*, *pkc1Δ*, *Cn sp1Δ::Cn SPI*, *pkc1Δ::pACT-Cn SPI*, and *Cn sp1Δ::pACT-PKC1* strains were grown on YPD + Sorbitol media, stained with India ink and observed under microscopy. *C.* Laccase activity- The above strains were plated following glucose starvation on ASN+ neuroepinephrine media and incubated overnight. *D.* Virulence of wt (H99), *Cn sp1Δ*, and *Cn sp1Δ::Cn SPI* strains were evaluated in a mice model following IV injection of 10⁶ cfu. * $p < 0.01$ for wt vs. *Cn sp1Δ* and *Cn sp1Δ::Cn SPI* vs. *Cn sp1Δ*; $p > 0.05$ for wt vs. *Cn sp1Δ::Cn SPI*.

Fig. 4. *Cn sp1Δ* and *pkc1Δ* share cell-wall integrity defects. wt (H99), *Cn sp1Δ*, *pkc1Δ*, *Cn sp1Δ::Cn SPI*, *pkc1Δ::PKC1*, *pkc1Δ::pACT-Cn SPI*, and *Cn sp1Δ::pACT-PKC1* strains were grown on YPD + Sorbitol media and suspended in PBS media to OD₆₀₀ of 0.1. Five 5-fold dilutions of each strain were spotted on

YPD+Sorbitol 1M agar plates with the various additives as described, and incubated in 30°C (except for the 37°C experiment) for 48 hours. CFW- calcofluor-white.

Fig. 5. Cn Sp1 is regulated by Pkc1. *A-C.* Cn *SP1* expression was assayed in wt and *pkc1Δ* strains, before (mid-log phase in YPD media) and following the detailed conditions by qRT-PCR. Relative expression was calculated using *ACT1* as reference gene. *D.* *c-myc* tagged Cn Sp1 (Cn *sp1Δ*: pACT -Cn *SP1*) and wt strains were grown to mid log phase in YPD and subjected to immunoprecipitation with anti *c-myc* antibody followed by western blotting with anti *c-myc* Ab. *E.* Cn *sp1Δ*: pACT-Cn *SP1* cells were grown to mid-log phase and immunoprecipitated following 1 hour induction in media containing the indicated condition (detailed in the 'Experimental Procedures'). Western blotting was done with either anti phosphorylated-T/S/Y or anti *c-myc* as loading control. Immunoprecipitated wt cells were used as negative control. *F.* Cn *sp1Δ*:GFP-Cn *SP1* strains were grown to mid-log phase and induced for 1 hour in media containing the indicated condition (detailed in the 'Experimental Procedures'). Representative pictures of Cn *sp1Δ*:GFP-Cn *SP1* cells before and following 1 hour induction are presented. DAPI was used for nuclear co-staining. *G.* Percentage of nuclear localization of GFP-Cn *SP1* before and after 30 and 60 minutes of induction (N = 300 cells).

Fig. 6. The Cn Sp1/Pkc1 pathway regulates gene expression following glucose starvation. *A.* Transcriptional profile of Cn *sp1Δ* (Y axis) and *pkc1Δ* (X axis) compared to wt following glucose starvation. Red dots: genes that are significantly downregulated in Cn *sp1Δ* and *pkc1Δ* (false discovery rate<0.05) compared to wt. Green dots: a subset of the genes labeled in red, that are also downregulated by at least 2-fold compared to wt (n=163). The genes in these groups are also presented in subsequent panels. *B.* Transcriptional profile of *pkc1Δ*:pACT-Cn *SP1* (compared to *pkc1Δ*) and *pkc1Δ* (compared to wt) following glucose starvation, presented in the Y and X axis, respectively. Green and red labels the same transcripts as in panel A. *C.* Transcriptional profile of wt (pre- and post-starvation) and *pkc1Δ* (compared to wt in starvation) presented in the Y and X axis, respectively. Green and red labels the same transcripts as in panel A. *D.* Pie diagram detailing the functional categories of 59 genes with known function, out of the 163 genes identified in panel A (green-labeled dots).

Fig. 7. Role of Sp1 in the pkc1 signaling pathway of *Cryptococcus neoformans*. Protein kinase C (Pkc1) phosphorylates members of the MAPK signaling pathway, Bck1 with subsequent phosphorylation of Mkk2 and the downstream component Mpk1 to mediated cell wall integrity, growth at high temperature and virulence. Pkc1 also regulates the transcription factor Sp1 by phosphorylation, leading to activation by nuclear translocation, as well as by transcriptional mechanisms, leading to regulation of osmoresistance, cell wall integrity and virulence in parallel to the MAPK pathway, as well as a unique pathway leading to resistance to nitrosative stress, capsule production and caspofungin resistance. Laccase (Lac1) is regulated by Pkc1 via an unknown pathway.

Strain	Temperature sensitivity (37°C)	India ink/ colony morphology	Melanin production	NaNO ₂ sensitivity	Cell wall inhibitor sensitivity ¹	Capofungin sensitivity	Cation sensitivity ²
Cn <i>sp1Δ</i>	wt	Hyper capsular/ mucoid	Moderately decreased	Moderate	Moderate	Profound	Moderate
Cn <i>sp1Δ</i>: pACT-<i>PKC1</i>	wt	Hyper capsular/ mucoid	Moderately decreased	Moderate	Moderate	Profound	Moderate
<i>pkc1Δ</i>	Profound	Aberrant/ mucoid	Profoundly decreased	Profound	Profound	Profound	Profound
<i>pkc1Δ</i>: pACT- Cn <i>SPI</i>	Profound	Aberrant/ dry, closer to wt	Profoundly decreased	Moderate	Moderate	Profound	Moderate

Table 1. Constituent expression of Cn *SPI* partially restores cell wall integrity in *pkc1Δ*. Phenotype is a comparison to wild type. ¹Sensitivity to 0.01% SDS, 0.5% Congo-red and 0.5 mg/ml calcoflour-white.

²Sensitivity to 200 mM CaCl₂ and 50 mM LiCl₂.

	Gene name	Cn <i>sp1Δ pkc1Δ</i> vs. wt		<i>pkc1Δ</i> :pACT-Cn <i>SP1</i> vs. <i>pkc1Δ</i>
Carbohydrate metabolism				
CNAG_05723	Alcohol dehydrogenase	-3.85	-3.01	2.89
CNAG_03785	α,α -trehalase	-1.25	-1.42	1.95
CNAG_02182	D-lactaldehyde dehydrogenase	-3.01	-4.74	1.81
CNAG_06672	Formate dehydrogenase	-3.27	-5.00	1.76
CNAG_00984	Glucose and ribitol dehydrogenase protein	-3.05	-3.36	1.41
CNAG_06374	Malate dehydrogenase	-1.95	-2.96	1.31
CNAG_04744	Mannose-6-phosphate isomerase	-1.57	-3.47	1.25
CNAG_02230	Phosphoketolase	-1.91	-3.36	1.17
CNAG_06169	R,R	-1.64	-2.51	0.87
CNAG_02000	Short-chain dehydrogenase	-2.80	-3.48	0.84
CNAG_03040	Transketolase	-1.31	-1.44	0.62
CNAG_00866	Transketolase	-2.27	-3.25	0.87
CNAG_02834	UDP-glucose:sterol glucosyltransferase	-1.42	-1.52	0.66
Membrane transporters/cnannels				
CNAG_04338	Cation diffusion facilitator 1	-1.08	-1.83	1.00
CNAG_06204	High-affinity nicotinic acid transporter	-1.66	-1.18	1.36
CNAG_01588	Hypothetical protein	-1.60	-2.63	1.73
CNAG_04416	Major facilitator superfamily transporter	-1.66	-2.09	0.78
CNAG_03502	Manganese resistance protein MNR2	-1.45	-2.26	1.04
CNAG_00905	MFS transporter	-1.03	-3.62	1.68
CNAG_01690	MFS transporter	-2.32	-5.10	2.22
CNAG_02527	Multidrug transporter	-1.71	-2.36	1.12
CNAG_05994	Multidrug transporter	-1.98	-3.15	1.38
CNAG_03824	Phosphate transport protein MIR1	-1.04	-2.31	1.00
CNAG_03432	Solute carrier family 2	-1.22	-1.52	0.61
CNAG_07874	Sugar transporter	-3.66	-5.44	1.33
CNAG_01742	Water channel	-2.30	-4.68	1.46
CNAG_04098	Xenobiotic-transporting ATPase	-1.59	-3.00	1.90
Stress response/peroxisomal metabolism				
CNAG_00575	Catalase 3	-2.99	-4.82	1.83
CNAG_04981	Catalase A	-1.44	-3.90	1.85
CNAG_01846	Flavoprotein	-1.71	-2.32	0.74
CNAG_02996	Flavoprotein oxygenase	-2.34	-2.19	0.84
CNAG_00315	HHE domain-containing protein	-2.45	-4.23	2.50
CNAG_03525	Trehalase	-1.72	-5.04	2.64

Lipids metabolism				
CNAG_03555	Acylglycerone-phosphate reductase	-2.16	-2.74	1.12
CNAG_02417	Lipase/esterase family protein	-1.46	-3.47	1.17
CNAG_07338	N-acyl-phosphatidylethanolamine-hydrolyzing phospholipase D	-1.39	-2.02	0.86
CNAG_04314	NAD+ kinase	-1.29	-3.51	1.39
CNAG_06594	Oxysterol binding protein	-1.07	-1.05	0.45
CNAG_04687	Stearoyl-CoA 9-desaturase	-1.37	-2.75	2.70
Amino acids metabolism				
CNAG_04417	2,4-dichlorophenoxyacetate alpha-ketoglutarate dioxygenase	-1.14	-4.19	3.25
CNAG_01912	Glutamine-dependent NAD(+) synthetase synthase	-1.24	-1.85	0.84
CNAG_00834	Phosphatidylserine decarboxylase	-2.50	-3.92	1.47
CNAG_06267	Rds1 protein	-1.62	-5.10	2.87
Transcriptional regulation/DNA repair				
CNAG_06602	Cysteine-type peptidase	-1.60	-2.77	0.97
CNAG_02690	Pirin	-1.47	-1.50	0.64
CNAG_05447	Pof4 protein	-1.23	-2.16	1.12
CNAG_05173	DNA-3-methyladenine glycosidase	-1.07	-1.65	0.58
Cell wall metabolism				
CNAG_06291	Deacetylase	-5.34	-3.11	2.09
CNAG_03771	DNA binding protein Ncp1	-1.41	-3.22	1.60
CNAG_05138	Exo-beta-1,3-glucanase	-1.28	-1.30	1.06
Protein synthesis and metabolism				
CNAG_05155	Protein-tyrosine-phosphatase	-2.07	-2.32	0.73
CNAG_02444	UPF0103 protein	-1.15	-2.09	1.08
Sulfur metabolism				
CNAG_04043	DUF636 domain-containing protein	-2.53	-3.01	1.10
CNAG_04206	DUF636 domain-containing protein	-2.08	-3.01	0.87
Miscellaneous				
CNAG_07800	Rop	-1.02	-1.06	0.44
CNAG_00254	NADH dehydrogenase	-1.09	-3.20	1.82
CNAG_07765	Bli-3 protein	-3.22	-5.33	1.88

Table 2. Cn Sp1/Pkc1 regulated genes. Summary of identifiable genes (n=59) downregulated in both Cn *sp1Δ* and *pkc1Δ* compared to wt under glucose starvation (>2 fold difference and FDR<0.05), divided by functional categories. Fold change in expression is presented in log₂. The fold change in gene expression in *pkc1Δ*:pACT-Cn *SP1* strain compared with *pkc1Δ* is also presented.

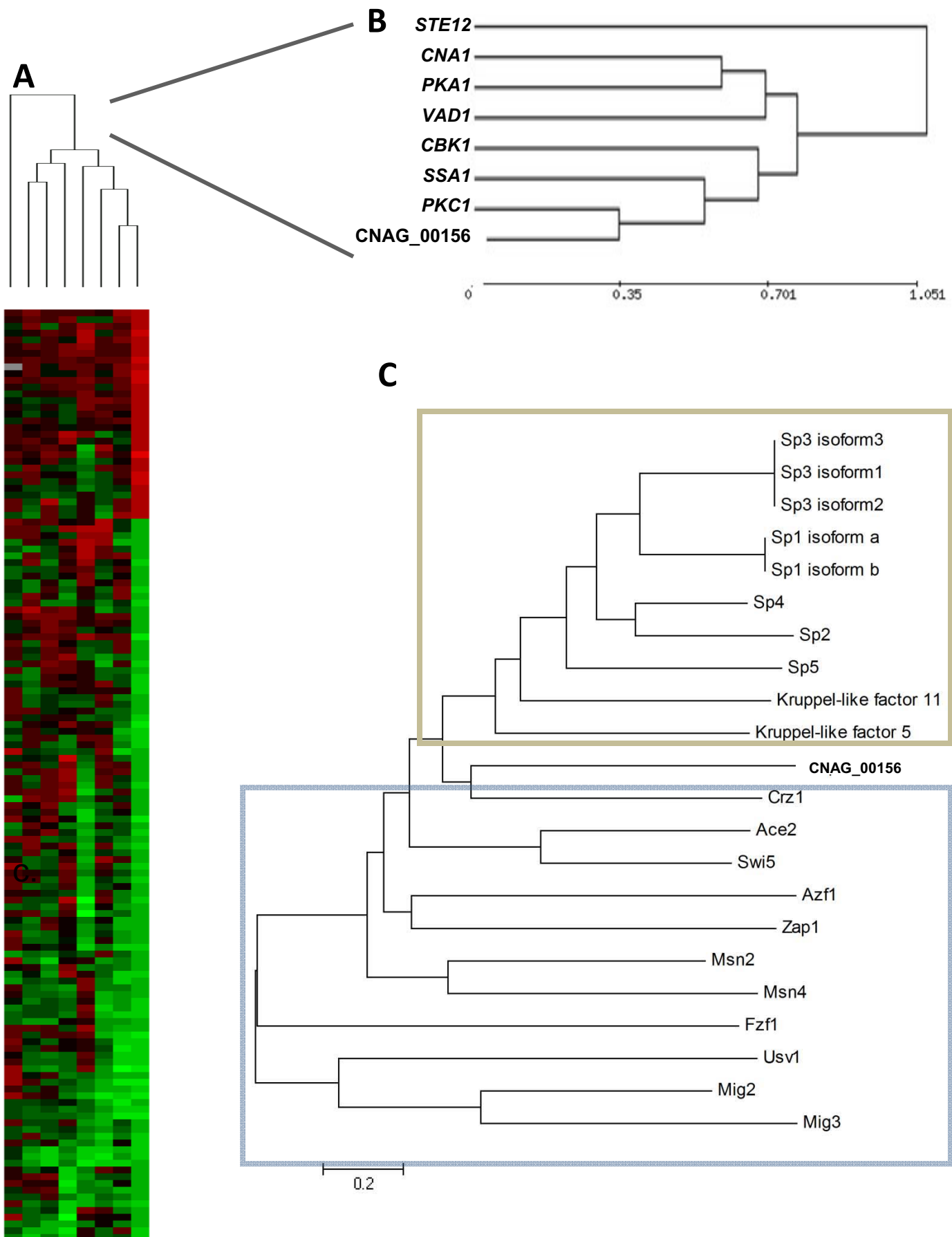
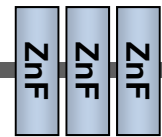


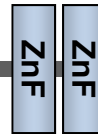
Figure 1

A

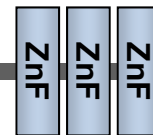
Cn Sp1 (*C. neoformans*)



Crz1 (*S. cerevisiae*)



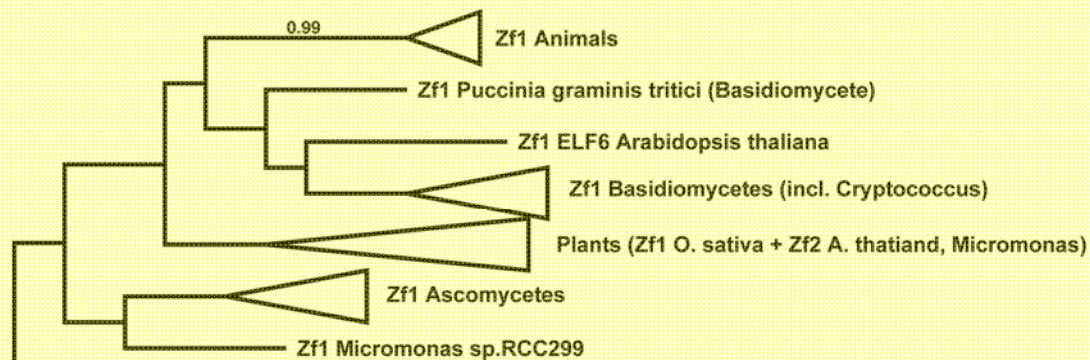
Sp1 (*H. sapiens*)



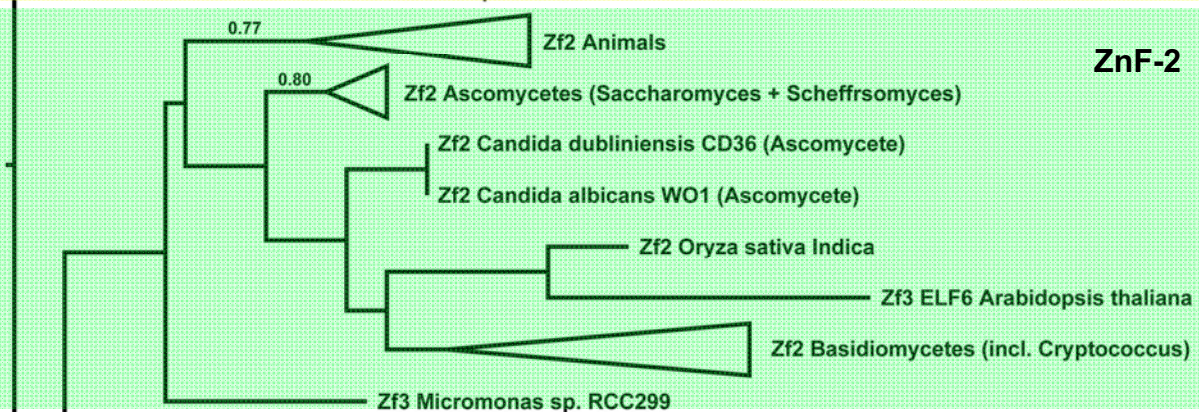
1 100 200 a.a.

B

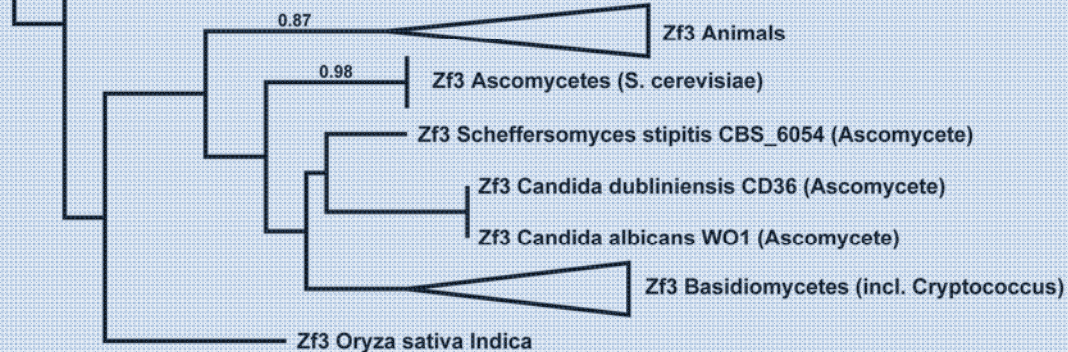
ZnF-1



ZnF-2



ZnF-3



7.0

Figure 2

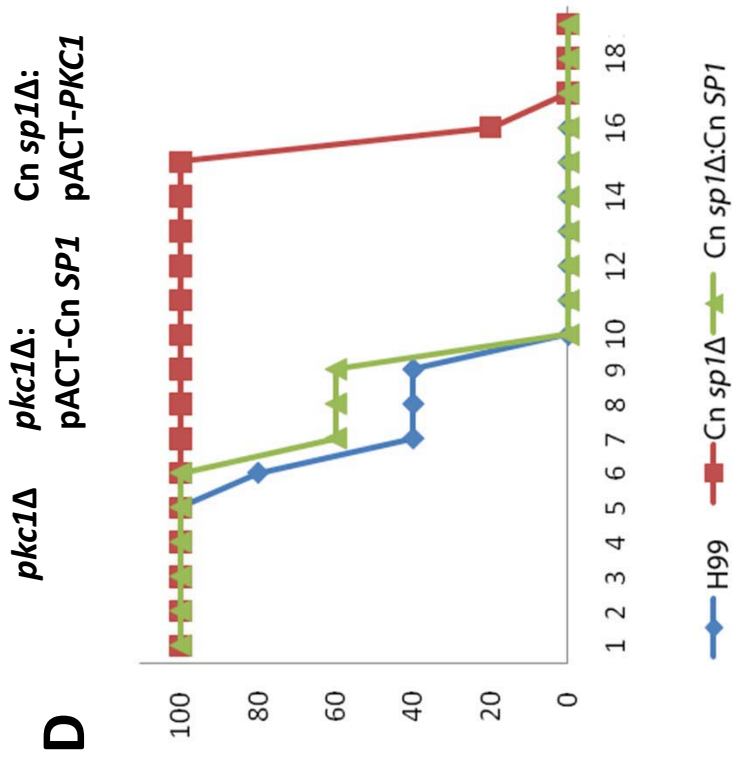
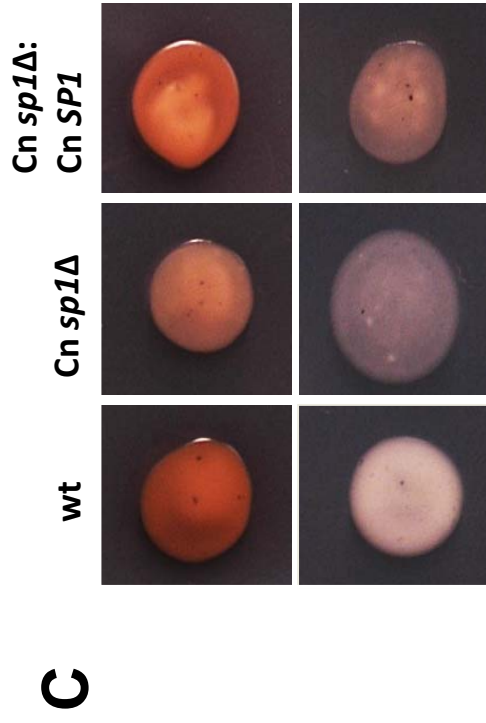
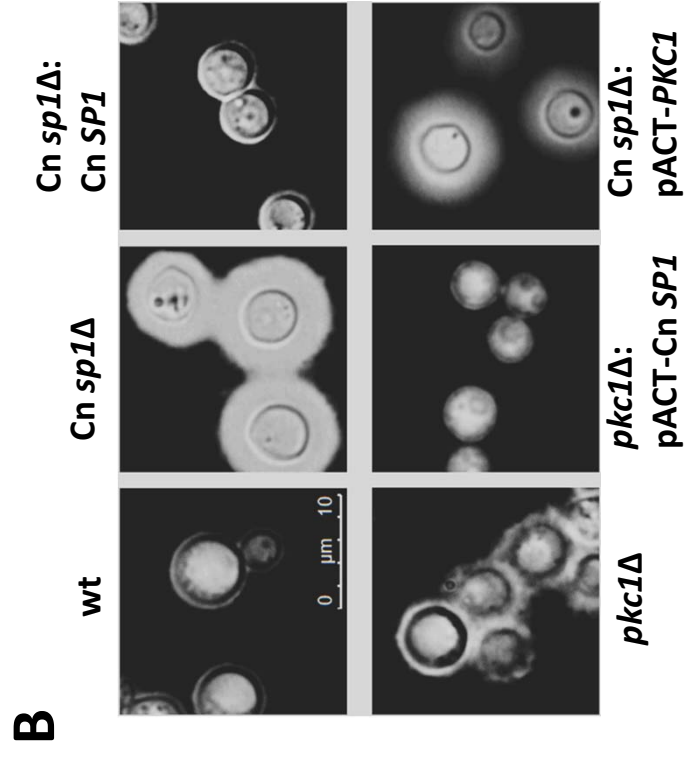
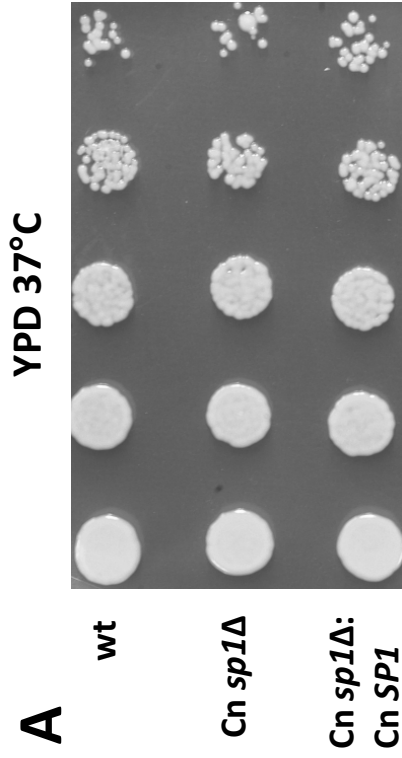


Figure 3

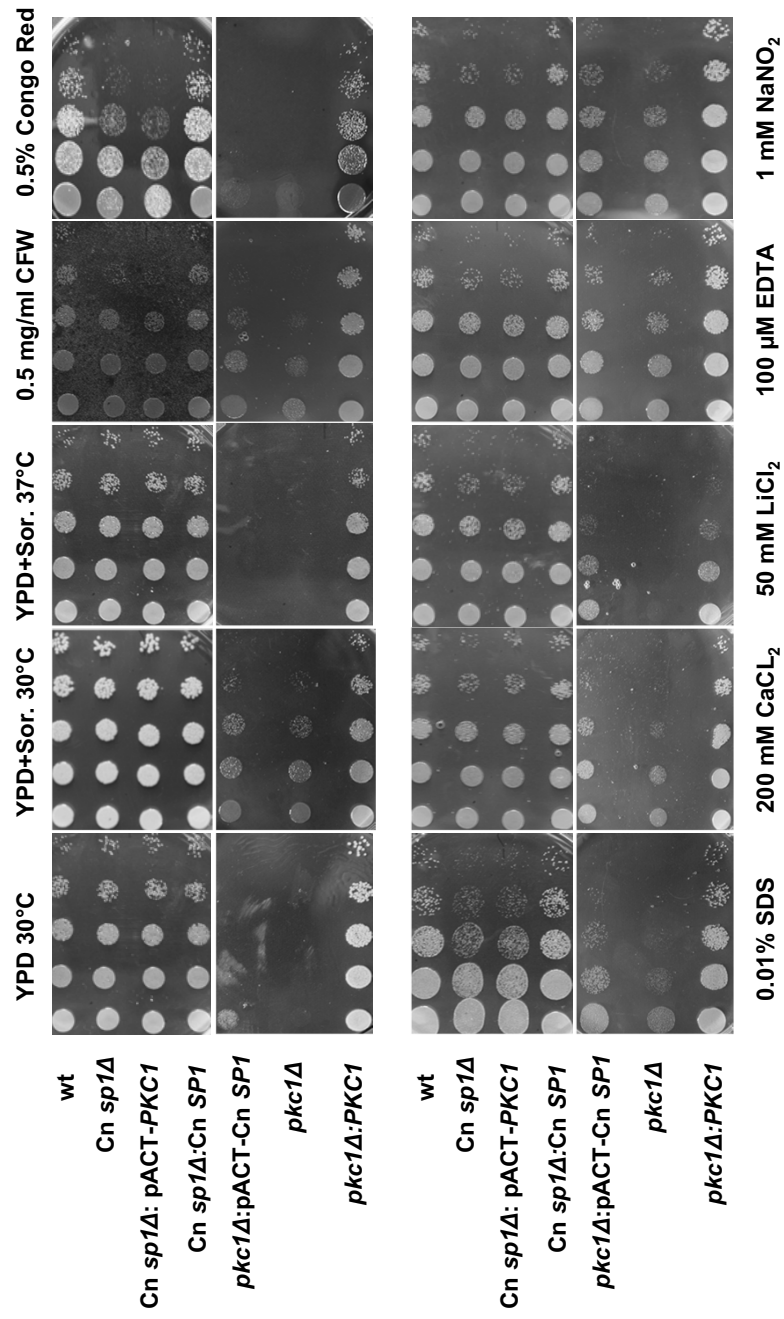


Figure 4

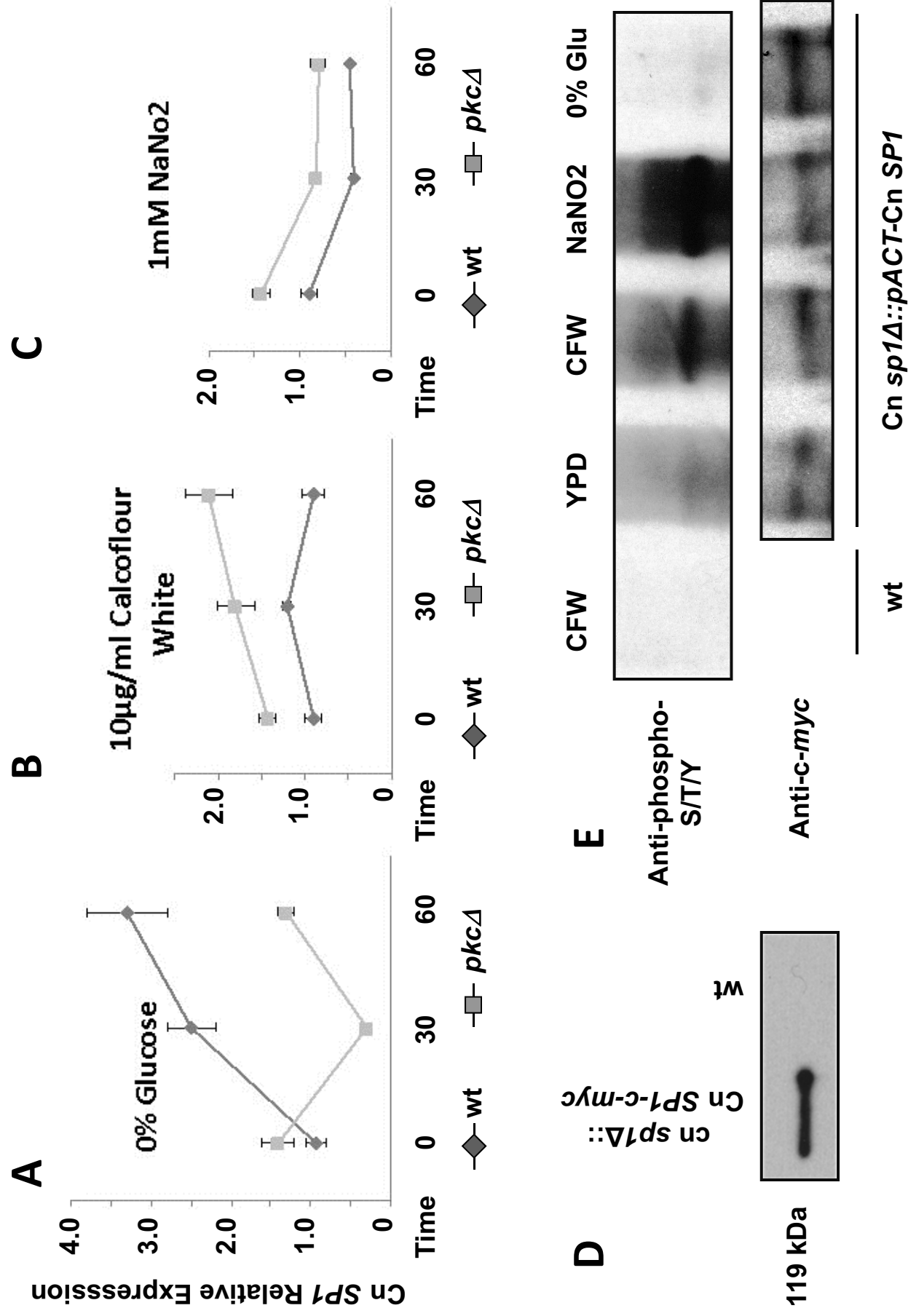
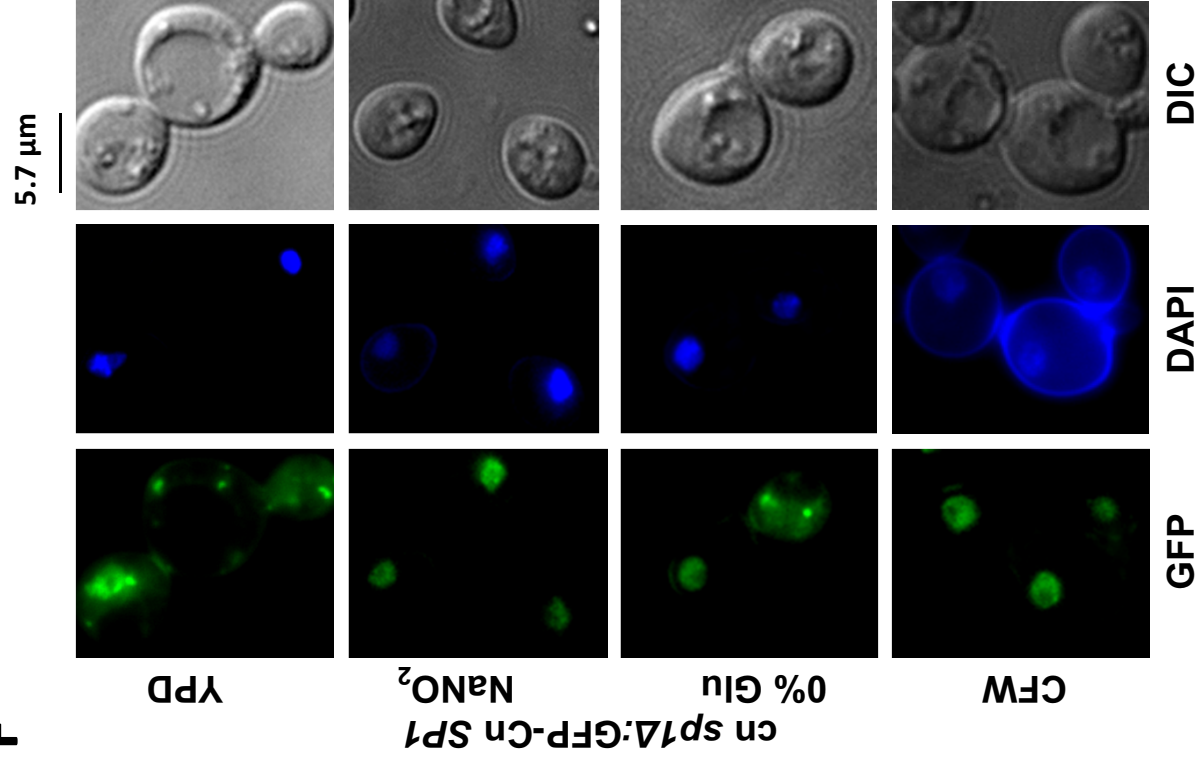
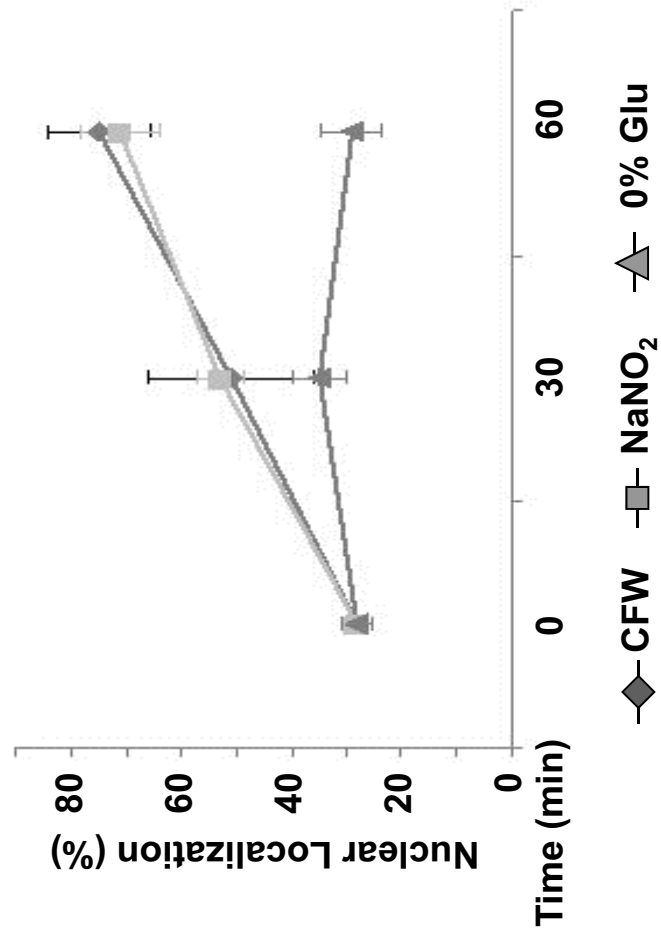
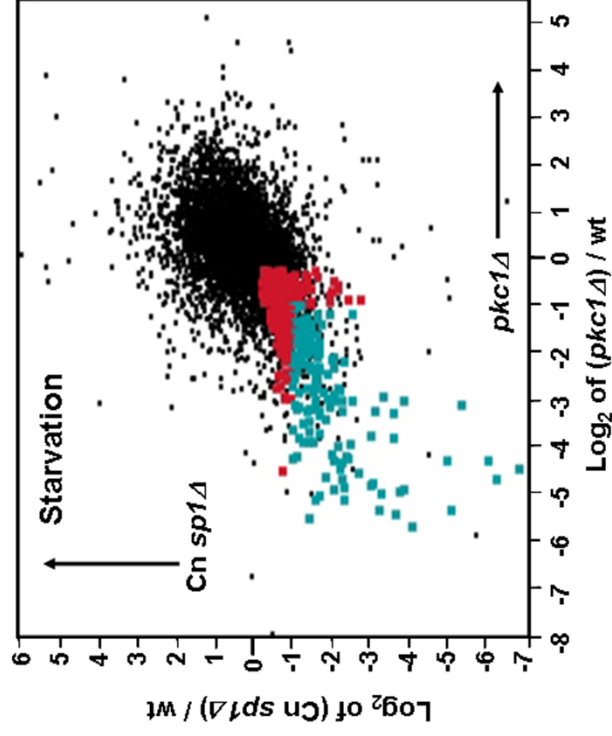


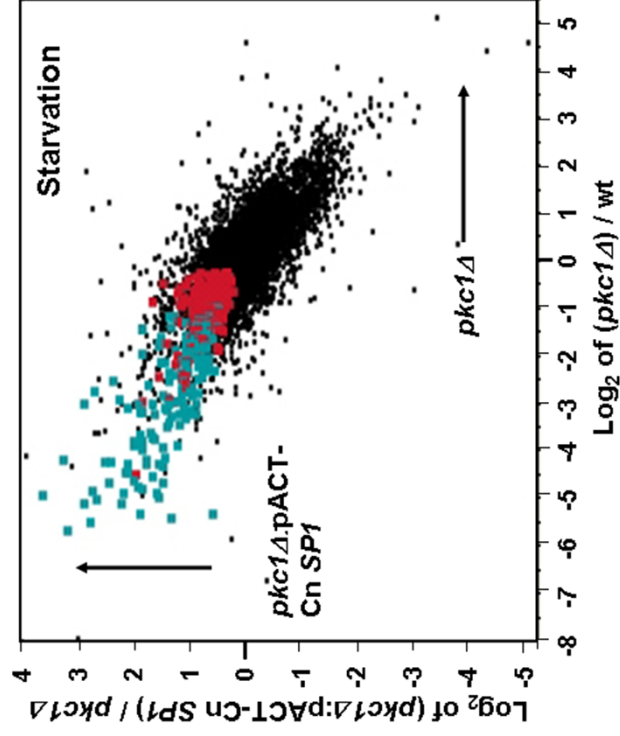
Figure 5

F**G****Figure 5**

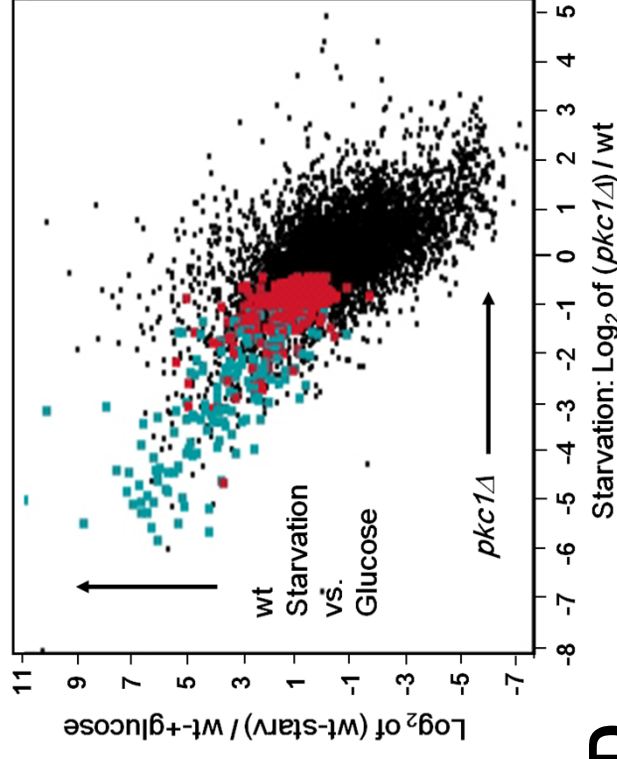
A



B



C



D

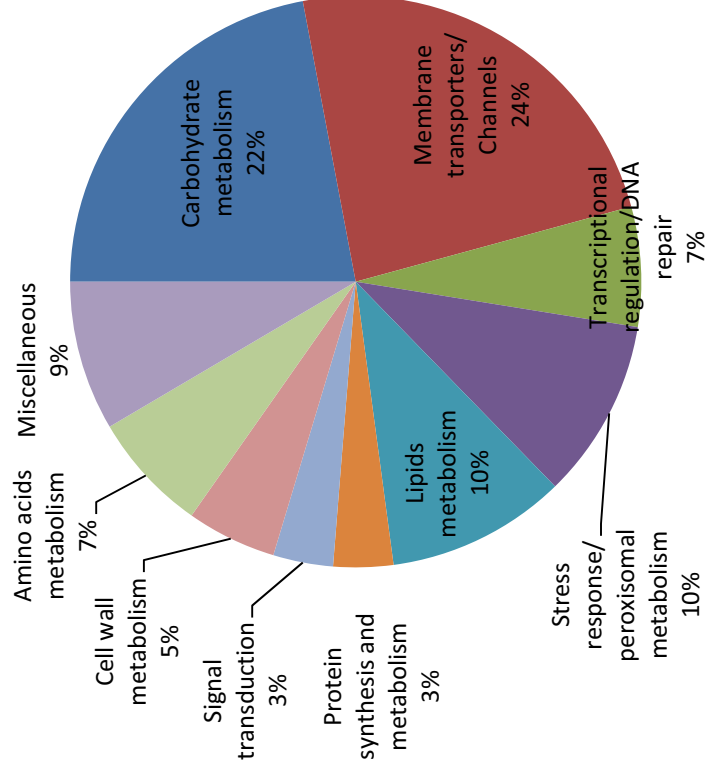


Figure 6

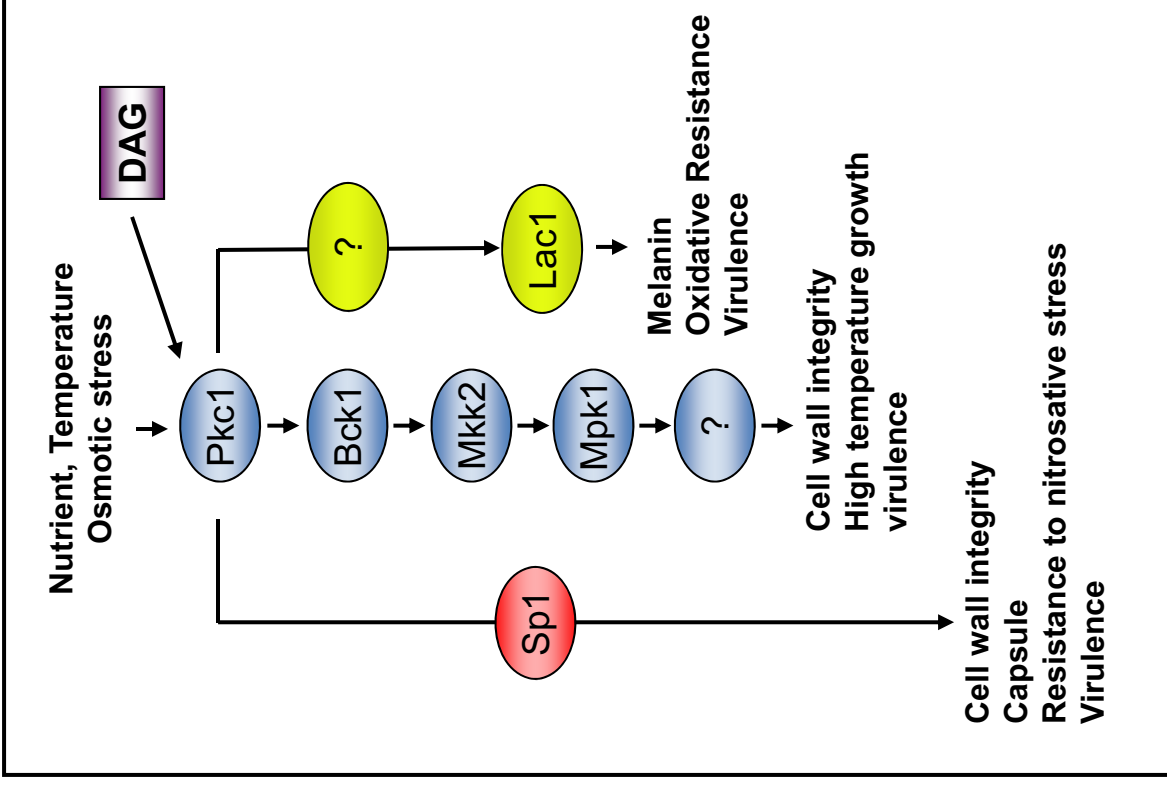


Figure 7

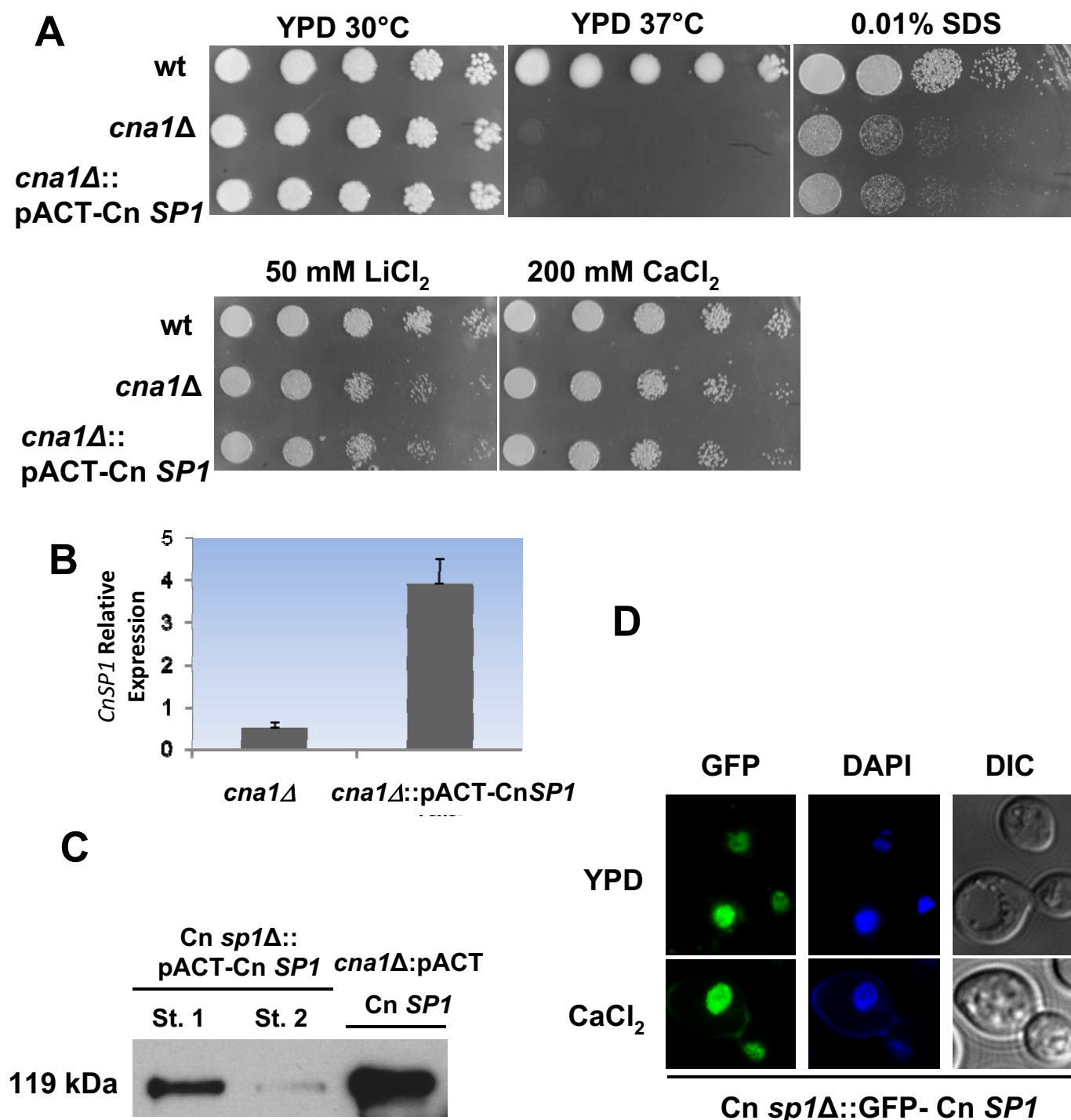


Figure S1. CNAG_00156 (Cn SP1) is not the *C. neoformans* CRZ1.

(A) WT, *cna1Δ*, and *cna1Δ*:pACT-Cn SP1 strains were grown on YPD + sorbitol media and suspended in PBS media to OD₆₀₀ of 0.1. Five 5-fold dilutions of each strain were spotted on the various media and observed for 48 hours. (B) shows validation by qRT-PCR of Cn SP1 over-expression in the *cna1Δ*:pACT-Cn SP1 strain. Values are ratios of expression of Cn SP1 transcript to ACT1.

(C) Cn *sp1Δ*:pACT-Cn SP1 (2 strains: st. 1 and St. 2) and *cna1Δ*:pACT-Cn SP1 strains (all containing a *c-myc* tag, see 'Experimental Procedures') were grown in YPD to an OD₆₀₀ of 0.4-0.6, lysed and immunoprecipitated with anti *c-myc* antibodies. Protein eluents were resolved on a SDS-PAGE gel. (D) Cn *sp1Δ*:GFP-Cn SP1 cells were grown in YPD to mid-log, and viewed with a confocal fluorescent microscope before and after addition of 20 mM CaCl₂. Nuclear localization of Cn Sp1 was observed independent of CaCl₂.

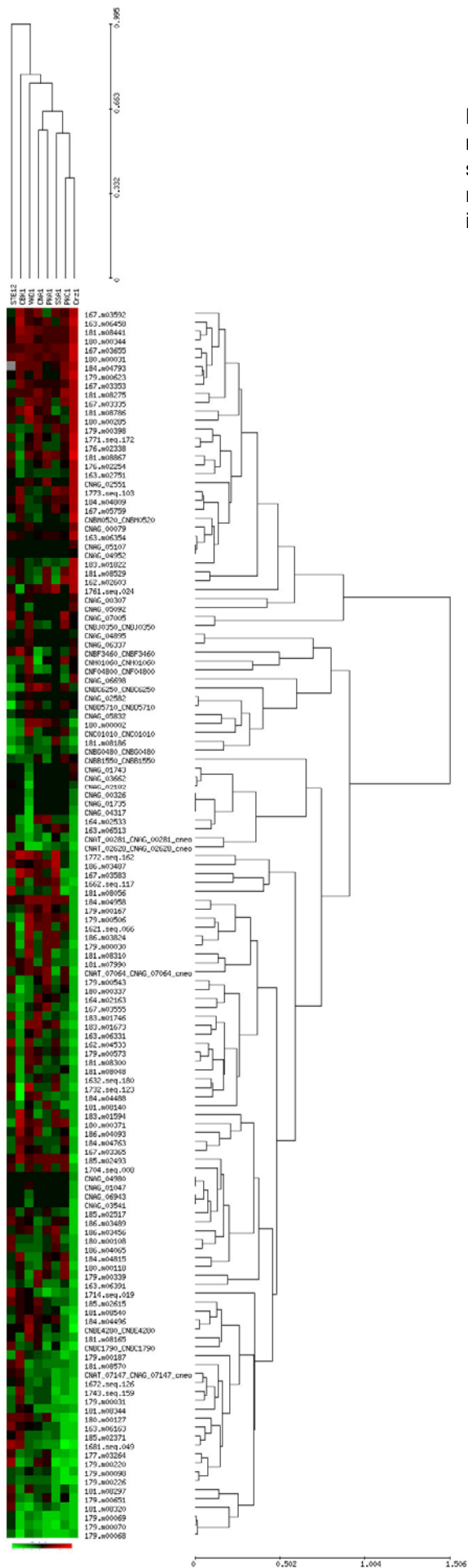


Figure S2: Transcriptional comparison of cryptococcal mutants under starvation conditions. Indicated strains were subjected to starvation and RNA prepared and subjected to microarray analysis using glass slide arrays as described in “Materials and Methods”.

Metazoan SP1-like ZF1, 2, and 3

	10	20	30	40	50
Zf1_SP1_HUMAN	HIC	-----HIQGC	GVK	-----Y	GKTSHLRAHLRWHHTGERP
Zf1_NP_651232_CG5669_Drosophila_melanogaster	HIC	-----HITGCHKV	-----	Y	GKTSHLRAHLRWHHTGERP
Zf1_XP_313726_AGAP004438_PA_Anopheles_gambiae_strPEST	HIC	-----HVSGCNKV	-----	Y	GKTSHLRAHLRWHHTGERP
Zf1_NP_997827_Sp1_Danio_rerio	HIC	-----HIPGCGKV	-----	Y	GKTSHLRAHLRWHHTGERP
Zf1_NP_001084888_Sp1_Xenopus_laevis	HIC	-----HIPGCGKV	-----	Y	GKTSHLRAHLRWHHTGERP
Zf1_NP_989935_Sp1_Gallus_gallus	HIC	-----HIPGCGKV	-----	Y	GKTSHLRAHLRWHHTGERP
Zf1_NP_038700_Sp1_Mus_musculus	HIC	-----HIQGC	GVK	-----Y	GKTSHLRAHLRWHHTGERP
Zf1_XP_002923324_Sp1_like_Ailuropoda_melanoleuca	HIC	-----HIQGC	GVK	-----Y	GKTSHLRAHLRWHHTGERP
Zf1_XP_543633_Sp1_iso1_Canis_familiaris	HIC	-----HIQGC	GVK	-----Y	GKTSHLRAHLRWHHTGERP
Zf1_XP_002711174_Sp1_Oryctolagus_cuniculus	HIC	-----HIQGC	GVK	-----Y	GKTSHLRAHLRWHHTGERP
Zf1_XP_002752575_Sp1_Callithrix_jacchus	HIC	-----HIQGC	GVK	-----Y	GKTSHLRAHLRWHHTGERP
Zf1_XP_001104948_Sp1_iso3_Macaca_mulatta	HIC	-----HIQGC	GVK	-----Y	GKTSHLRAHLRWHHTGERP
Zf1_NP_001071495_Sp1_Bos_taurus	HIC	-----HMQGC	GVK	-----Y	GKTSHLRAHLRWHHTGERP
Zf1_XP_001926920_Sp1_Sus_scrofa	HIC	-----HMQGC	GVK	-----Y	GKTSHLRAHLRWHHTGERP
Zf1_XP_001370863_similar_Sp4_Monodelphis_domestica	HIC	-----HIEGC	GVK	-----Y	GKTSHLRAHLRWHHTGERP
Zf1_EFP83209_hypo_PGTG09162_Puccinia_graminis_tritici_CRL_75367003	YIC	-----EMCGES	-----	F	TRRYNLRHGQRAHKGKPK
Zf1_XP_566613_hypo_prot_Cryptococcus_neoformans_neoformans_JEC21	FKC	-----PVPGCGST	-----F	TRHFN	LKGHLRSHNDERP
Zf1_XP_778140_CNBA1400_Cryptococcus_neoformans_neoformans_B3501A	FKC	-----PVPGCGST	-----F	TRHFN	LKGHLRSHNDERP
Zf1_XP_761291_hypo_prote_UM05144_Ustilago_maydis_521	FAC	-----PIPGCGST	-----	F	TRQYNLRGHLRSHADERP
Zf1_XP_001731547_hypo_pro_MGL_1730_Malassezia_globosa_CBS_7966	FTC	-----PFDCGST	-----	F	TRQYNLRGHLRSHADERP
Zf1_EDV12282_transcr_reg_CRZ1_Saccharomyces_cerevisiae_RM11_1a	FAC	-----DVCGKK	-----	F	TRPYNLKSHLRTHTNERP
Zf1_EEU04771_Crz1p_Saccharomyces_cerevisiae_JAY291	FAC	-----DVCGKK	-----F	TRPYNLK	SHLRTHTNERP
Zf1_CAY82170_Crz1p_Saccharomyces_cerevisiae_EC1118	FAC	-----DVCGKK	-----F	TRPYNLK	SHLRTHTNERP
Zf1_EDN62786_transcr_factor_Saccharomyces_cerevisiae_YJM789	FAC	-----DVCGKK	-----	F	TRPYNLKSHLRTHTNERP
Zf1_NP_014371_Crz1p_Saccharomyces_cerevisiae_S288c	FAC	-----DVCGKK	-----	F	TRPYNLKSHLRTHTNERP
Zf1_XP_001382598_zf_C2H2_Scheffersomyces_stipitis_CBS_6054	YAC	-----HLC	DKR	-----F	TRPYNLKSHLRTHTNERP
Zf1_XP_002419476_transcr_reg_putative_Candida_dubliniensis_CD36	YAC	-----HLC	DKR	-----F	TRPYNLKSHLRTHTNERP
Zf1_EEQ44614_cons_hypo_pro_Candida_albicans_WO1	YAC	-----HLC	DKR	-----F	TRPYNLKSHLRTHTNERP
Zf1_NP_196044_ELF6_Arabidopsis_thaliana	CTH	-----EGCGK	-----	F	RAHKLVLHQRVHKDERP
Zf1_XP_002508356_pred_protein_Micromonas_sp_RCC299	FAC	-----PAPGCLNA	-----	F	SNAYDLRHSVTHSDERP
Zf1_EAY96228_hypothro_Osl_18121_Oryza_sativa_Indica	FIC	-----SYENCGKT	-----	F	VDVAALRKHVHNFRQ
Zf2_EFP83209_hypo_PGTG09162_Puccinia_graminis_tritici_CRL_75367003	FAC	-----GYPGCTSR	-----	F	ARAHQDKRHYKLHLGVKD
Zf2_XP_761291_hypo_prote_UM05144_Ustilago_maydis_521	YKC	-----DWP	GCEKS	-----F	ARSHDCKRQHLNLNPK
Zf2_XP_001731547_hypo_pro_MGL_1730_Malassezia_globosa_CBS_7966	FKC	-----EWP	GCGRS	-----F	ARSHDCKRQHLNLNPK
Zf2_XP_566613_hypo_prot_Cryptococcus_neoformans_neoformans_JEC21	FKC	-----LYEGCPKA	-----F	ARSHDCKRQHLNLNPK	-----F
Zf2_XP_778140_CNBA1400_Cryptococcus_neoformans_neoformans_B3501A	FKC	-----LYEGCPKA	-----F	ARSHDCKRQHLNLNPK	-----F
Zf2_XP_002419476_transcr_reg_putative_Candida_dubliniensis_CD36	FIC	-----SKCGKS	-----	F	ARSHDCKRQHLNLNPK
Zf2_EEQ44614_cons_hypo_pro_Candida_albicans_WO1	FIC	-----SKCGKS	-----	F	ARSHDCKRQHLNLNPK
Zf2_EDV12282_transcr_reg_CRZ1_Saccharomyces_cerevisiae_RM11_1a	FIC	-----SICGKA	-----	F	ARSHDCKRQHLNLNPK
Zf2_EEU04771_Crz1p_Saccharomyces_cerevisiae_JAY291	FIC	-----SICGKA	-----F	ARSHDCKRQHLNLNPK	-----F
Zf2_CAY82170_Crz1p_Saccharomyces_cerevisiae_EC1118	FIC	-----SICGKA	-----F	ARSHDCKRQHLNLNPK	-----F
Zf2_EDN62786_transcr_factor_Saccharomyces_cerevisiae_YJM789	FIC	-----SICGKA	-----	F	ARSHDCKRQHLNLNPK
Zf2_NP_014371_Crz1p_Saccharomyces_cerevisiae_S288c	FIC	-----SICGKA	-----	F	ARSHDCKRQHLNLNPK
Zf2_XP_001382598_zf_C2H2_Scheffersomyces_stipitis_CBS_6054	FIC	-----NVCGKA	-----	F	ARSHDCKRQHLNLNPK
Zf2_SP1_HUMAN	FMG	-----TWSYCGKR	-----F	TRSD	ELQRHRTHTGEKK
Zf2_NP_651232_CG5669_Drosophila_melanogaster	FVC	-----SWA	FCGKR	-----F	TRSD
Zf2_XP_313726_AGAP004438_PA_Anopheles_gambiae_strPEST	FIC	-----NWG	TCGKR	-----F	TRSD
Zf2_NP_997827_Sp1_Danio_rerio	FVC	-----SWF	CGKR	-----F	TRSD
Zf2_NP_001084888_Sp1_Xenopus_laevis	FVC	-----TWV	FCGKR	-----F	TRSD
Zf2_NP_989935_Sp1_Gallus_gallus	FIC	-----GWM	LCGKR	-----F	TRSD
Zf2_NP_038700_Sp1_Mus_musculus	FMG	-----NWSY	CGKR	-----F	TRSD
Zf2_XP_002923324_Sp1_like_Ailuropoda_melanoleuca	FMG	-----TWSY	CGKR	-----F	TRSD
Zf2_XP_543633_Sp1_iso1_Canis_familiaris	FMG	-----TWSY	CGKR	-----F	TRSD
Zf2_XP_002711174_Sp1_Oryctolagus_cuniculus	FMG	-----TWSY	CGKR	-----F	TRSD
Zf2_XP_002752575_Sp1_Callithrix_jacchus	FMG	-----TWSY	CGKR	-----F	TRSD
Zf2_XP_001104948_Sp1_iso3_Macaca_mulatta	FMG	-----TWSY	CGKR	-----F	TRSD
Zf2_NP_001071495_Sp1_Bos_taurus	FMG	-----TWSY	CGKR	-----F	TRSD
Zf2_XP_001926920_Sp1_Sus_scrofa	FMG	-----TWSY	CGKR	-----F	TRSD
Zf2_XP_001370863_similar_Sp4_Monodelphis_domestica	FVC	-----NWI	FCGKR	-----F	TRSD
Zf2_NP_196044_ELF6_Arabidopsis_thaliana	FEC	-----SWK	GCSMT	-----F	TRSD
Zf2_XP_002508356_pred_protein_Micromonas_sp_RCC299	FAC	-----KTC	GKT	-----F	TRSD
Zf2_EAY96228_hypothro_Osl_18121_Oryza_sativa_Indica	YIC	-----QEP	GCGKR	-----F	TRSD
Zf3_SP1_HUMAN	FAC	-----PECPKR	-----F	MRSD	HLKSHIKTHQNKKG
Zf3_NP_651232_CG5669_Drosophila_melanogaster	FQC	-----QEC	NKK	-----F	MRSD
Zf3_XP_313726_AGAP004438_PA_Anopheles_gambiae_strPEST	FIC	-----VFC	NKK	-----F	MRSD
Zf3_NP_997827_Sp1_Danio_rerio	FIC	-----TECPKR	-----	F	MRSDHLKSHIKTHQNKKG
Zf3_NP_001084888_Sp1_Xenopus_laevis	FIC	-----PECPKR	-----	F	MRSDHLKSHIKTHQNKKG
Zf3_NP_989935_Sp1_Gallus_gallus	FAC	-----PECPKR	-----	F	MRSDHLKSHIKTHQNKKG
Zf3_NP_038700_Sp1_Mus_musculus	FAC	-----PECPKR	-----	F	MRSDHLKSHIKTHQNKKG
Zf3_XP_002923324_Sp1_like_Ailuropoda_melanoleuca	FAC	-----PECPKR	-----	F	MRSDHLKSHIKTHQNKKG
Zf3_XP_543633_Sp1_iso1_Canis_familiaris	FAC	-----PECPKR	-----	F	MRSDHLKSHIKTHQNKKG
Zf3_XP_002711174_Sp1_Oryctolagus_cuniculus	FAC	-----PECPKR	-----	F	MRSDHLKSHIKTHQNKKG
Zf3_XP_002752575_Sp1_Callithrix_jacchus	FAC	-----PECPKR	-----	F	MRSDHLKSHIKTHQNKKG
Zf3_XP_001104948_Sp1_iso3_Macaca_mulatta	FAC	-----PECPKR	-----	F	MRSDHLKSHIKTHQNKKG
Zf3_NP_001071495_Sp1_Bos_taurus	FAC	-----PECPKR	-----	F	MRSDHLKSHIKTHQNKKG
Zf3_XP_001926920_Sp1_Sus_scrofa	FAC	-----PECPKR	-----	F	MRSDHLKSHIKTHQNKKG
Zf3_XP_001370863_similar_Sp4_Monodelphis_domestica	FEC	-----PEC	SKR	-----F	MRSD
Zf3_EFP83209_hypo_PGTG09162_Puccinia_graminis_tritici_CRL_75367003	YSC	-----PVC	CRKT	-----F	MRSD
Zf3_XP_761291_hypo_prote_UM05144_Ustilago_maydis_521	HTC	-----EQCGKT	-----	F	MRSDHLKSHIKTHQNKKG
Zf3_XP_001731547_hypo_pro_MGL_1730_Malassezia_globosa_CBS_7966	YQC	-----ESC	GKT	-----F	MRSD
Zf3_XP_566613_hypo_prot_Cryptococcus_neoformans_neoformans_JEC21	FEC	-----EGCGKK	-----F	MRSD	HLKSHIKTHQNKKG
Zf3_XP_778140_CNBA1400_Cryptococcus_neoformans_neoformans_B3501A	FEC	-----EGCGKK	-----F	MRSD	HLKSHIKTHQNKKG
Zf3_EDV12282_transcr_reg_CRZ1_Saccharomyces_cerevisiae_RM11_1a	YVCGGK	LKDGP	PWCGGKK	-----	FARSDALGRHFKTESGRR
Zf3_EEU04771_Crz1p_Saccharomyces_cerevisiae_JAY291	YVCGGK	LKDGP	PWCGGKK	-----F	MRSD
Zf3_CAY82170_Crz1p_Saccharomyces_cerevisiae_EC1118	YVCGGK	LKDGP	PWCGGKK	-----F	MRSD
Zf3_EDN62786_transcr_factor_Saccharomyces_cerevisiae_YJM789	YVCGGK	LKDGP	PWCGGKK	-----	FARSDALGRHFKTESGRR
Zf3_NP_014371_Crz1p_Saccharomyces_cerevisiae_S288c	YVCGGK	LKDGP	PWCGGKK	-----	FARSDALGRHFKTESGRR
Zf3_XP_002419476_transcr_reg_putative_Candida_dubliniensis_CD36	FKCEGY	LQDGT	RWCGGKS	-----	FARSDALGRHFKTESGRR
Zf3_EEQ44614_cons_hypo_pro_Candida_albicans_WO1	FKCEGY	LQDGT	RWCGGKS	-----	FARSDALGRHFKTESGRR
Zf3_XP_001382598_zf_C2H2_Scheffersomyces_stipitis_CBS_6054	FOCKG	FLKSGK	PWCGGKR	-----	FARSDALGRHFKTESGRR
Zf3_NP_196044_ELF6_Arabidopsis_thaliana	YIC	-----KVD	GCL	-----F	MRSD
Zf3_XP_002508356_pred_protein_Micromonas_sp_RCC299	FKC	-----EHP	GCGKL	-----F	MRSD
Zf3_EAY96228_hypothro_Osl_18121_Oryza_sativa_Indica	FIC	-----PHPGCGKA	-----	F	MRSDHLKSHIKTHQNKKG

Figure S3a: Sequence alignment of Zn finger regions and associated sequences of fungi and metazoans
Representative Sp1, Crz1 and Cn Sp1-like protein sequences were retrieved from a BLASTp (ref) search. Full protein sequences were aligned using the MUSCLE software (ref) and individual zinc-finger motifs were identified and extracted. A multiple sequence alignment of the three zinc-finger motifs was created manually based on the MUSCLE alignment.

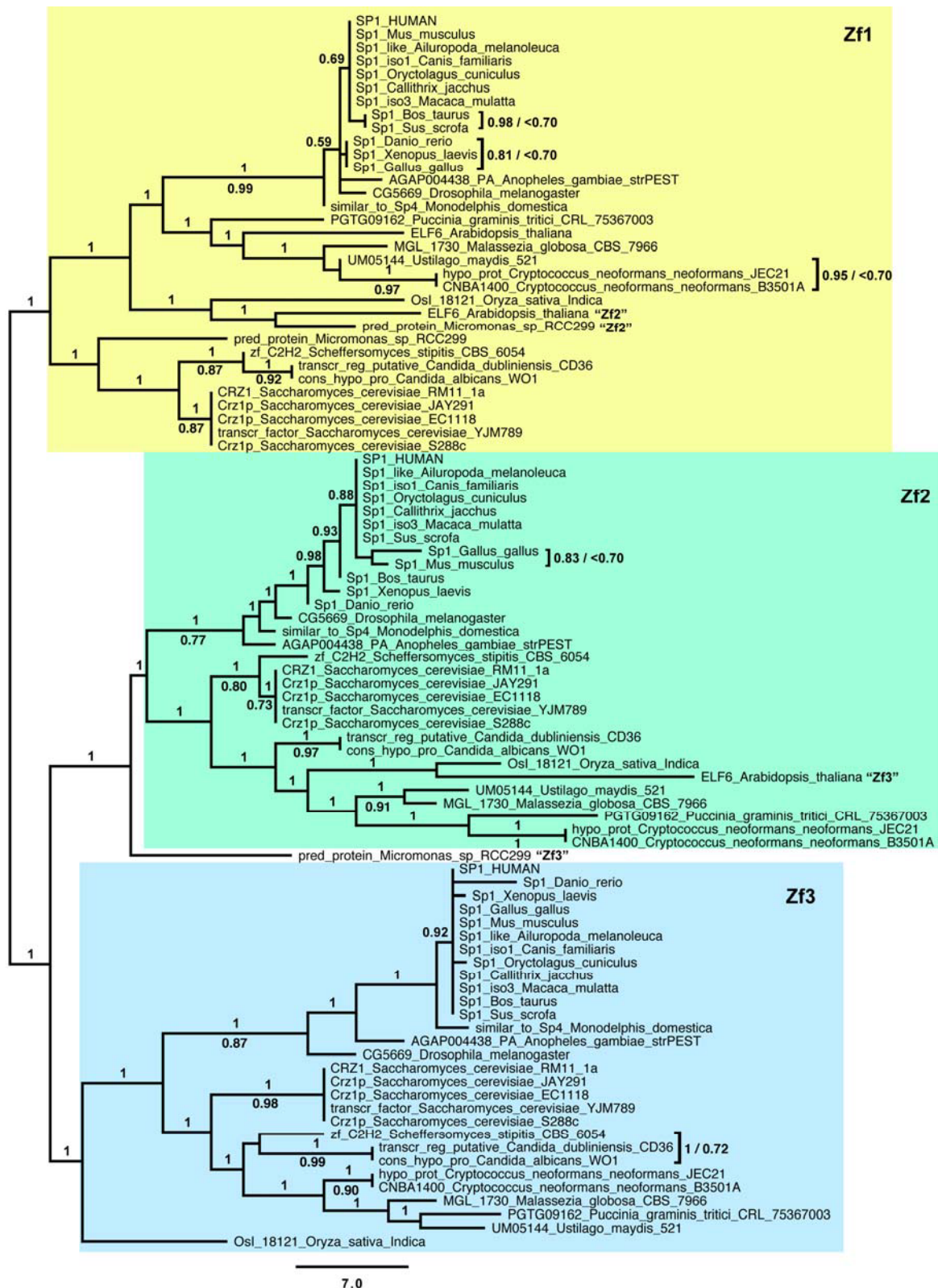


Figure S3b: Parimonious trees constructed from sequences aligned in Figure S3a. Sequences from Figure S3a were submitted to PAUP (ref) and a heuristic search for the most parsimonious tree was performed. PAUP found 500 equally parsimonious trees. To ascertain the level of phylogenetic support in the data 500 nonparametric bootstrap replicates were generated and their consensus calculated. The 50% majority-rule consensus of the 500 equally parsimonious trees is given in Figure S3b. Groups are collapsed when they are found in fewer than 50% of the equally parsimonious trees. The numbers above the branches represent the frequency of that group among the equally parsimonious trees. The numbers below the branches (or to the right of the sequence IDs when internal branches were short) are the bootstrap support percentages. Bootstrap support values less than 70% are not shown.

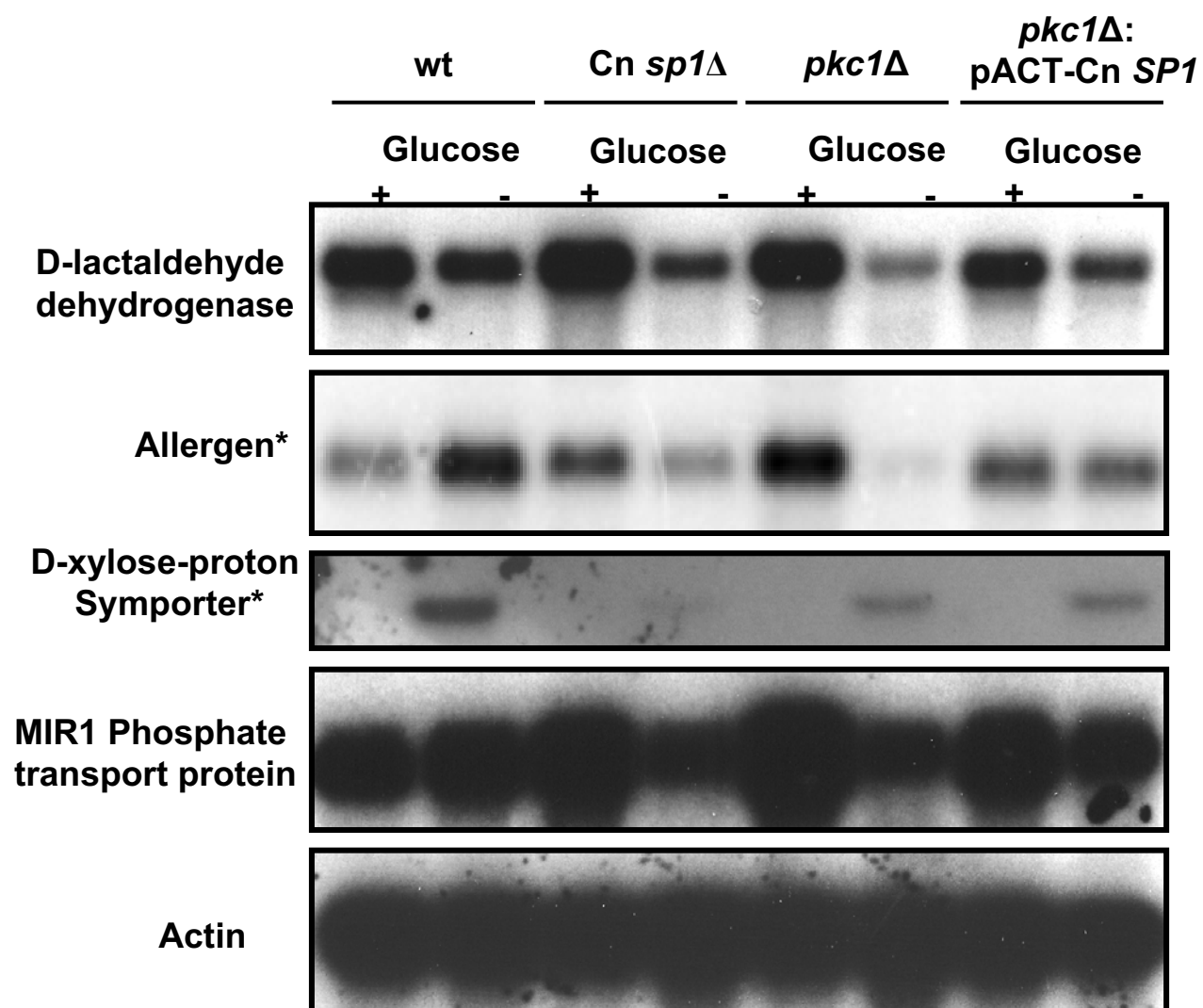


Figure S4a. Northern blot validation of genes in microarray experiments.

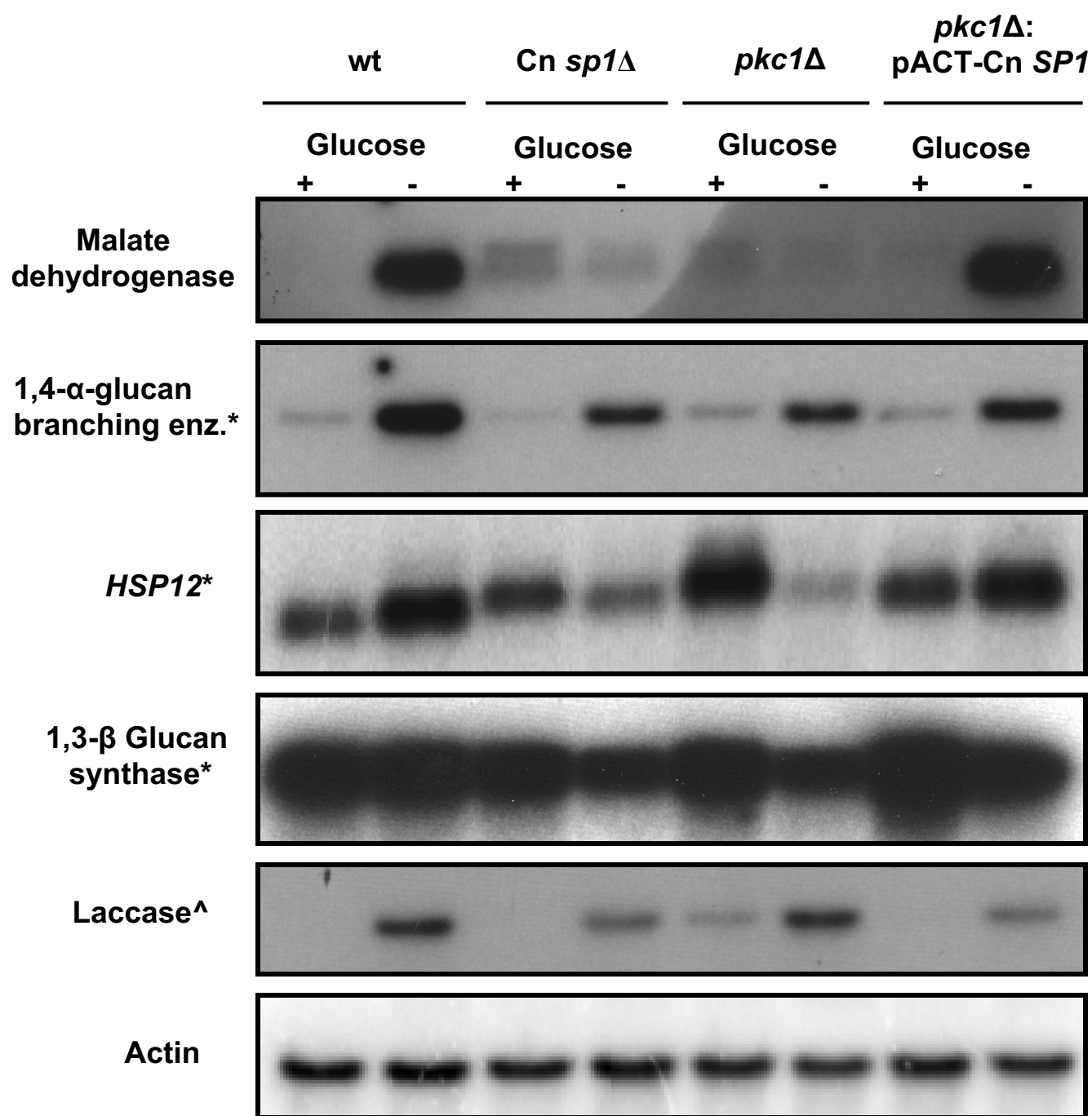


Figure S4a. Northern blot validation of genes in microarray experiments.

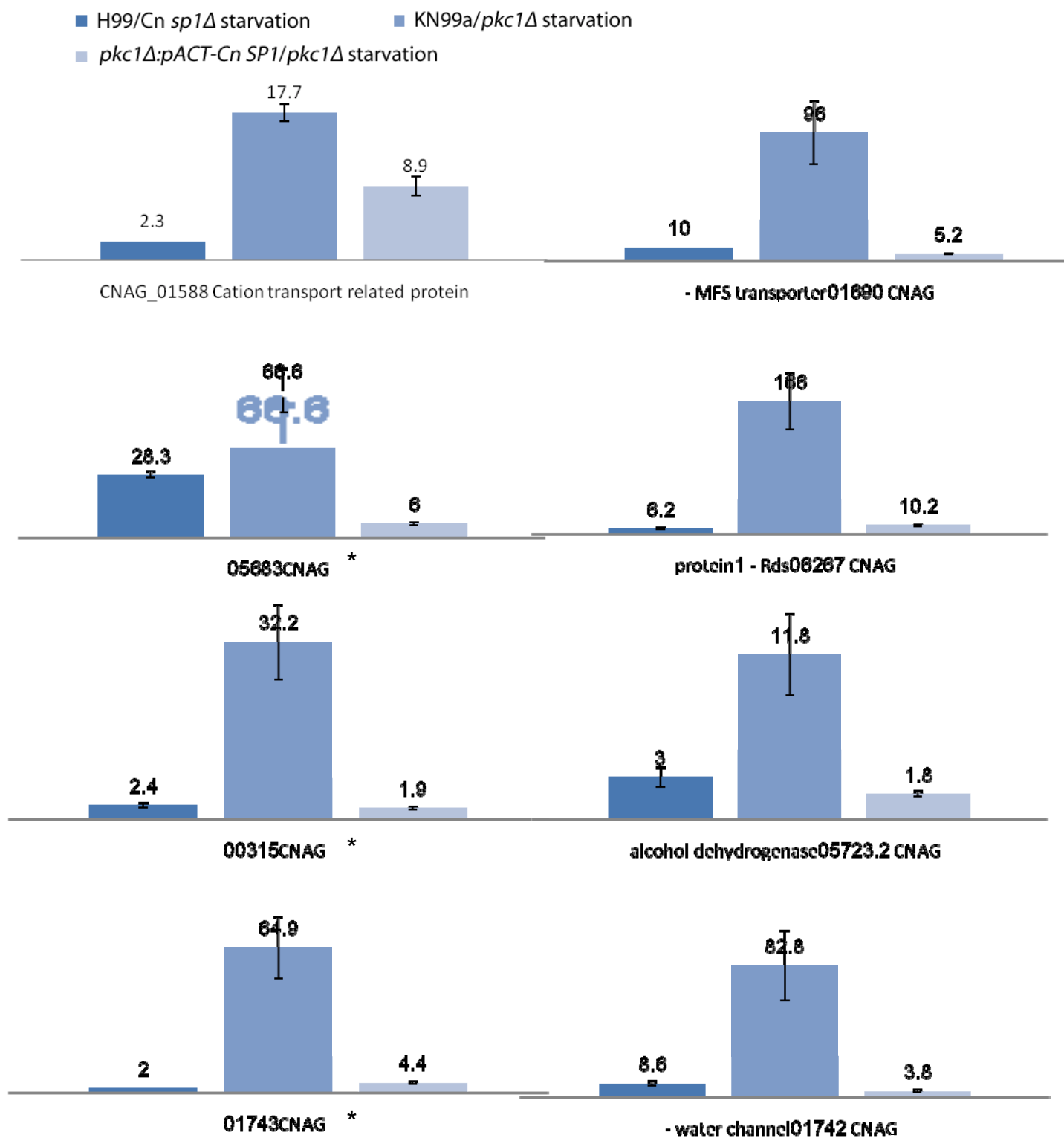


Figure S4b. qRT-PCR validation of genes in microarray experiments.

Results represent normalized expression ($\Delta\Delta C_t \pm$ SD) in starvation of the following strains/conditions (with *ACT1* as control): wt (H99)/Cn *sp1*Δ, wt (KN99)/*pkc1*Δ, and *pkc1*Δ:pACT-Cn *SP1*/*pkc1*Δ.

*Denotes genes that were identified in both microarray studies. NAD-dependent malic enzyme had an FDR of >0.05 but was also chosen based on interest.

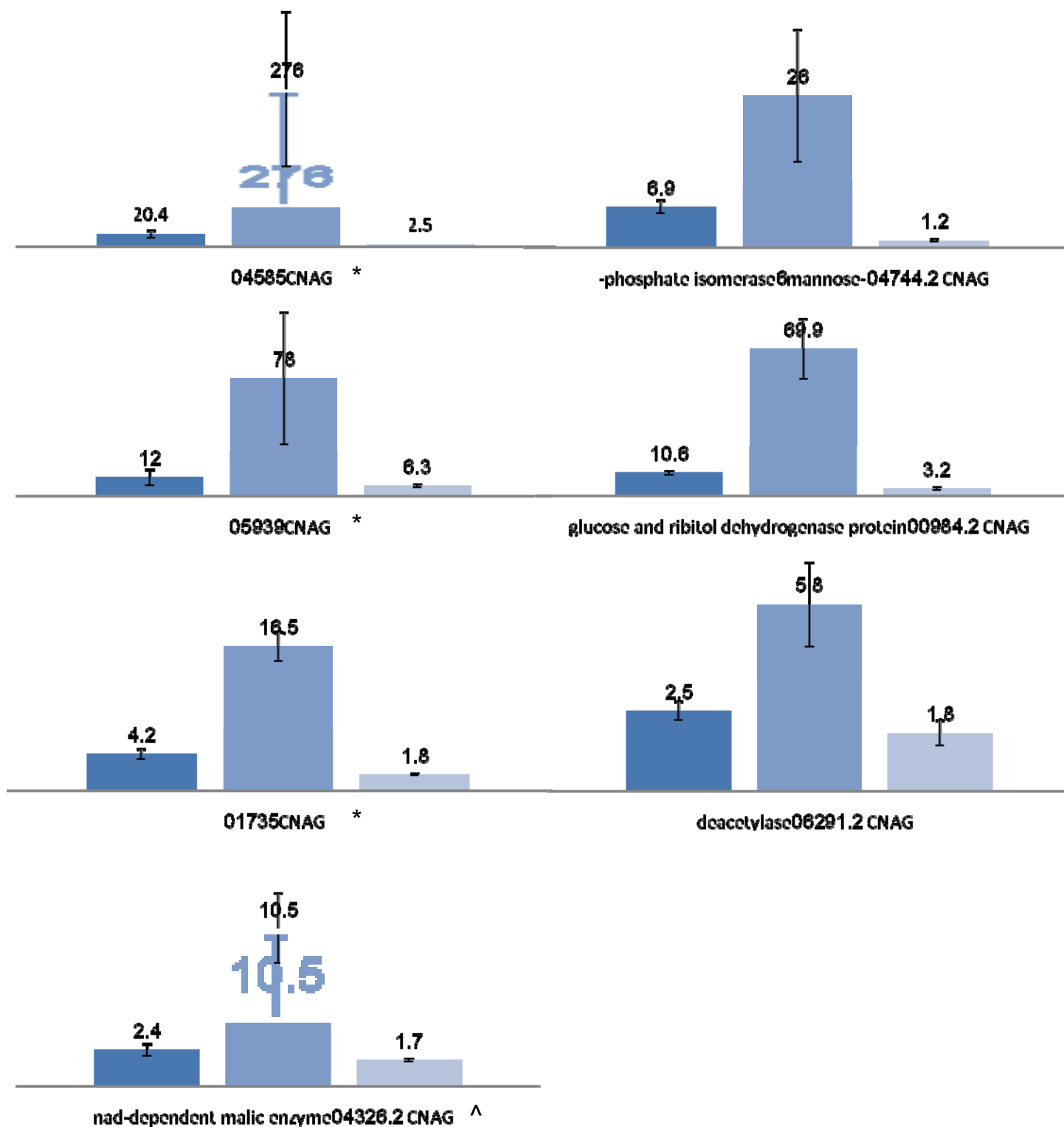


Figure S4b (con't)

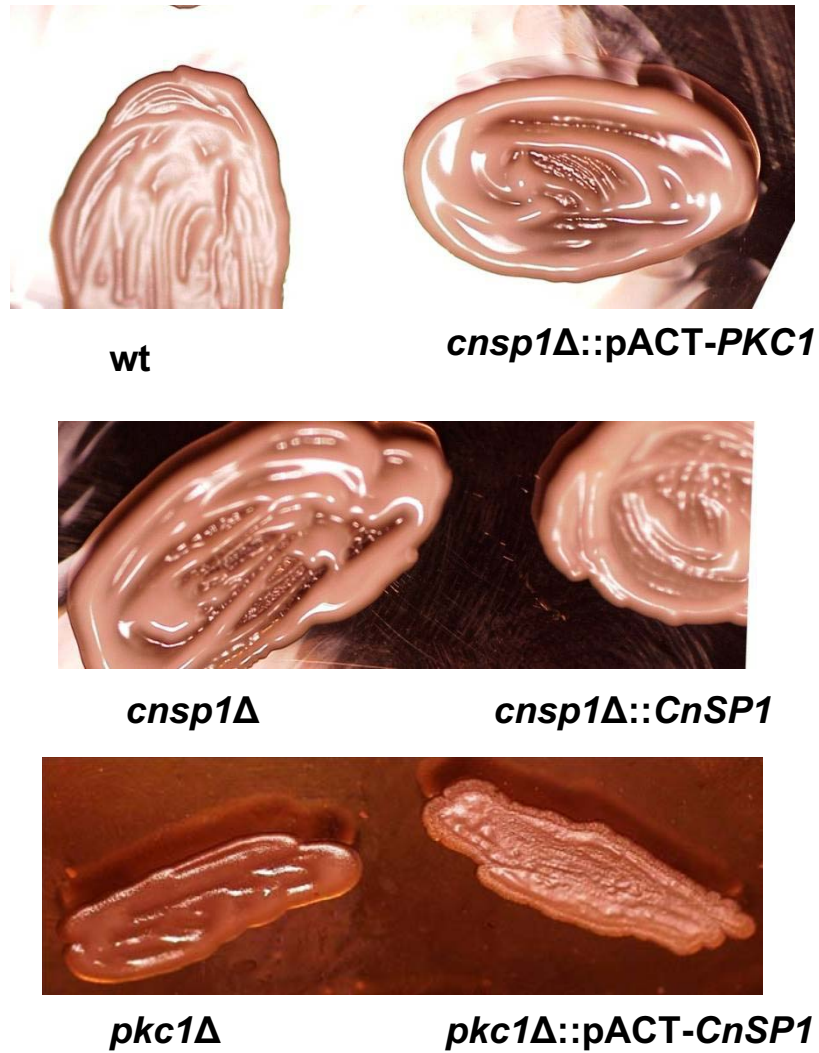


Figure S5. *Cn sp1Δ* (*cnag00156Δ*) and *pkc1Δ* demonstrates mucoid morphology . WT (H99), *cnag00156Δ* (designated *Cn sp1Δ*), *pkc1Δ*, *Cn sp1Δ::Cn SP1*, *pkc1Δ::pACT-Cn SP1*, and *Cn sp1Δ::pACT-PKC1* strains were grown on YPD + Sorbitol media (non-capsule inducing condition) and photographed.

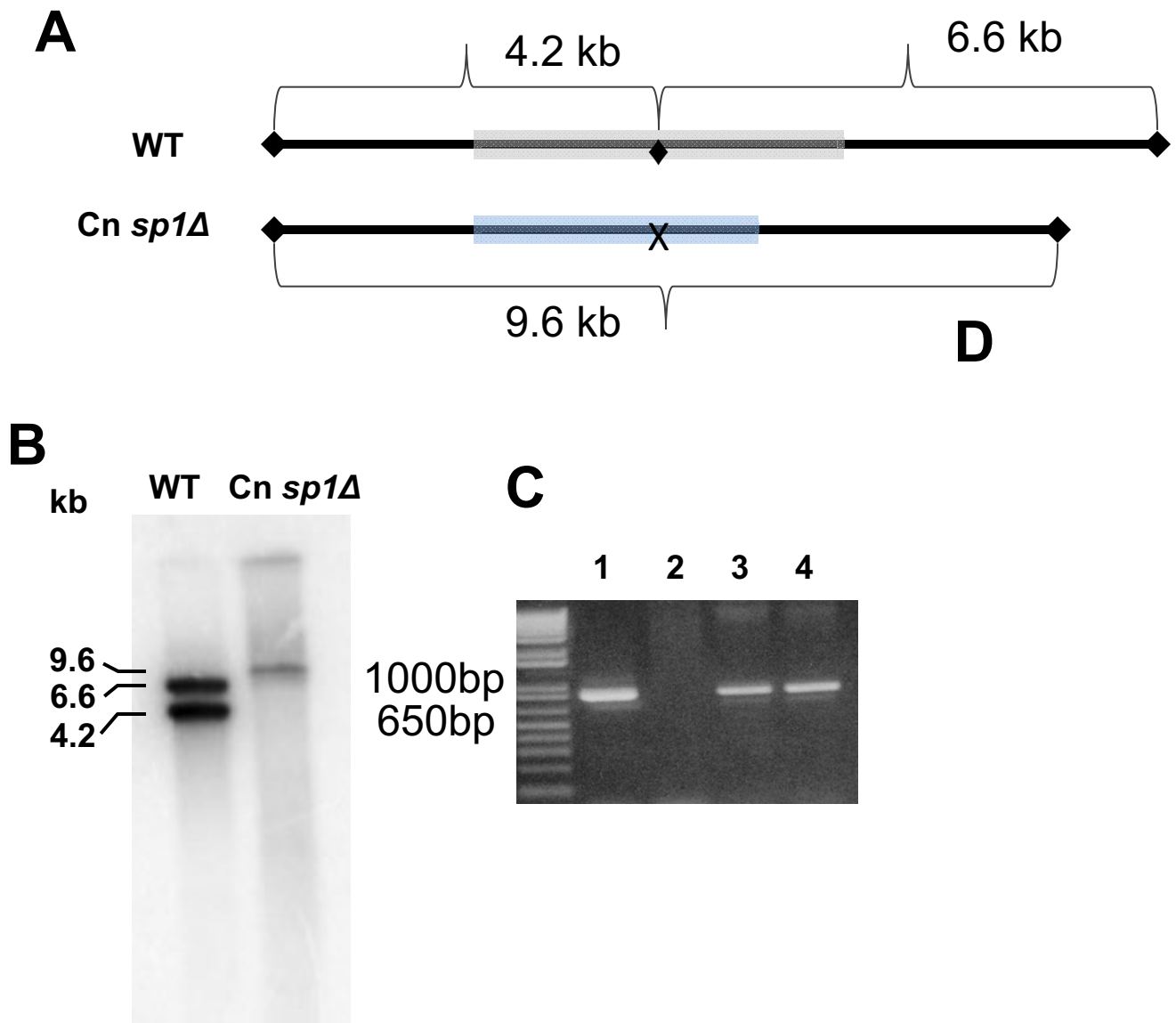


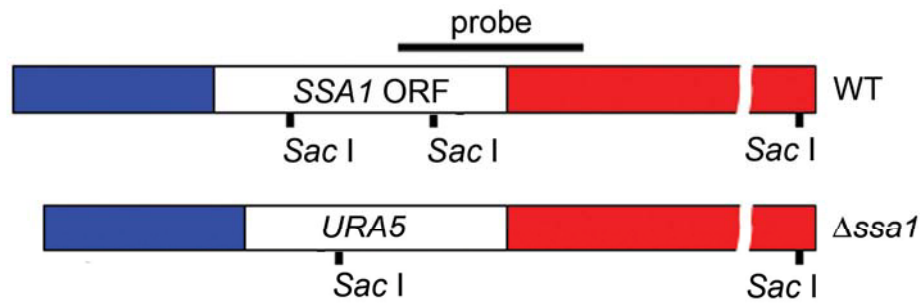
Figure S6. Generation of Cn *SP1* knockout and its complementation.

(A) Map WT vs. Cn *sp1Δ* genetic regions. *MunI* sites are marked with a diamond sign. Cn *SP1* coding region and knockout construct are marked with grey and blue, respectively. **(B)** Southern blot of wt and Cn *sp1Δ* strains digested with *MunI*. Hybridization fragment included the 1st and last 500bp of the Cn *SP1* coding region (primers detailed in 'experimental procedures'), to allow detection of both WT and mutant. In the WT fragment, a *MunI* site, located 2076bp into the ORF lead to detection of 2 separate bands. In Cn *sp1Δ*, the WT ORF was replaced with a ~2.4 construct lacking a *MunI* site (marked 'x'), leading to only one band.

(C) Lack of Cn *SP1* transcript in Cn *sp1Δ*. DNase-treated RNA was extracted from H99 (lanes 1,3) and Cn *sp1Δ* (lanes 2,4) cells, followed by reverse transcription and PCR of Cn *SP1* (lanes 1,2) and *SSA1* (lanes 3,4) as control. Cn *SP1* cDNA is amplified in H99 but not in Cn *sp1Δ*.

(D) Southern blot (uncut) of Cn *sp1Δ* complementation demonstrates episomal location of Cn *SP1* expression construct in two strains (lane 1 and lane 2). Probe of Cn *SP1* was design to detect a fragment not present in the mutant, using primers Crz1probe 1608S (5'- CCACAATCCCATCCTTTACCAC) and Crz1probe 2465A (5'- AACCGACTTACCCGCAAACG). Lane 1-WT; 2-5-complemented strains; 6- Cn *sp1Δ*. Genomic DNA localized in reference to Ethidium bromide-stained gel.

A



B

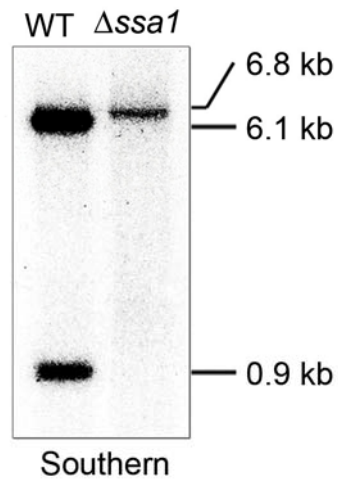


Figure S7. Generation of *SSA1* knockout strain.

(A) Schematic drawing of the *SSA1* locus in the WT and the *ssa1* Δ strains, outlining the location of the Southern blot probe shown in B and *SacI* restriction sites.

(B) *SacI*-cut Southern blot of the WT and the *ssa1* Δ strains, probed to the location outlined in A.

Strain Name	Source
H99	Kindly provided by J. Perfect
H99 FOA	Erickson et al., 2001
KN99a	Kindly provided by J. Lodge
Cn <i>sp1</i> Δ	This study
Cn <i>sp1</i> Δ:Cn <i>SP1</i>	This study
<i>ssa1</i> Δ	This study
<i>pkc1</i> Δ	Gerick et al., 2008
<i>pkc1</i> Δ: <i>PKC1</i>	Gerick et al., 2008
<i>pka1</i> Δ	Hicks et al., 2004
<i>vad1</i> Δ	Panepinto et al., 2005
<i>cbk1</i> Δ	Walton et al., 2006
<i>cna1</i> Δ	Odom et al., 1997
<i>stel2</i> Δ	Yue et al., 1999
Cn <i>sp1</i> Δ:pACT- <i>PKC1</i>	This study
Cn <i>sp1</i> Δ:pACT-Cn <i>SP1</i>	This study
<i>cna1</i> Δ:pACT-Cn <i>SP1</i>	This study
<i>pkc1</i> Δ:pACT-Cn <i>SP1</i>	This study
Cn <i>sp1</i> Δ:GFP-Cn <i>SP1</i>	This study

Table S1. Strains used in this study

Supplemental Methods:

Generation of a SSA1 knockout strain-Standard methods were used for disruption of the *SSA1* gene, as described previously (Hu et al., 2008). Briefly, to make the deletion construct, 2 PCR-amplified fragments of the Cn *SSA1* (using primers *SSA1*-up-*Xba* I-s, 5'-TTATCTAGACTTGAACGTAAA GCTAAGAG, and *SSA1*-up-*Bgl* II-a, 5'-TAAAGATCTTTATCTATTAAAGCTTTG AG; *SSA1*-down-*Eco*R I-s, AGCGAATTCCAAGGCGTAGTAATAAAAGG, and *SSA1*-down-*Xho* I-a, 5'-TATCTCGAGTGTGACGAGAGAGATGGAG), the first digested with *Xba* I and *Bgl* II and the second digested with *Eco*R I and *Xho* I, was mixed with a 1.3-kb PCR fragment of the *C. neoformans URA5* gene described previously (Hu et al., 2008), digested with *Bgl* II and *Eco*R I and ligated to BlueScript SK digested with *Xba* I and *Xho* I. The final disruption allele with a 1.3-kb *URA5* marker flanked on either side by a 500-bp DNA sequence homologous to genomic regions of the *SSA1* gene was PCR-amplified and introduced into H99FOA cells via a biolistic approach (Cox et al., 1996) to effect a 2.2-kb deletion within the *SSA1* coding region. Transformants were screened for potential *SSA1* deletion mutant by a PCR, and the specific disruption of the *SSA1* gene in candidate mutant was verified by Southern blot analysis (Figure S6b).

Construction and use of an H99 three probe microarray: Construction and use of an H99 two-probe microarray: *Cryptococcus neoformans* var *grubii* H99 transcript sequences were downloaded from the BROAD Institute website. Hybridization probe sequences(60-mer) were selected using e-Array software (Agilent): two for each of the 6,969 transcripts, one of them strongly 3-prime biased ("best probe methodology") the other less so ("best distribution methodology"). The 13,938 unique probes were arrayed in 3 replicate, randomized, locations on the Agilent Sure-Print microarray slide, 4x44K format. Additional control probes were included as well. (This array design has been deposited in GEO, accession GPL11486, as well as the mAdb NIH microarray database, internal name "Cnda"). Cy dye labeled hybridization target material was prepared from 10 ug total RNA and hybridized at 65o C for 17 hrs using TECAN 4800 HS Pro robotic hybridization station operating "Agilent GE 17 hrs" program. Slides were dried and maintained under nitrogen until scanning at 5 um resolution using Agilent G2505C. Agilent Feature Extraction software (protocol GE2_107_Sep09) was used for image analysis. Co-hybridizations were performed according to a common reference design with pooled sample in Cy5 channel on each array. Replicate RNA samples from two independent experiments for each condition. SAS and JMP-Genomics software (SAS, Cary NC) was used for statistical analysis. Starting with Agilent Feature Extraction "processed signal" (normalized) data, one channel per sample, we calculated the median signal for each locus ID (3 replicates of 2 unique probes) and transformed to log2. A mixed effects ANOVA model (fixed effect of strain-condition, random effect of array_ID) was computed for each gene over 24 different strain/growth conditions, and expression difference estimates calculated for the comparisons of interest. False Discovery Rate (FDR) estimates were based on the raw p-values for the 6,969 gene-wise tests over 5 treatment group comparisons. The genes called significantly different with FDR of 0.05 had a raw p-value < 0.03.